A pathway in quiescent cells that controls p27Kip1 stability, subcellular localization, and tumor suppression

Arnaud Besson, Mark Gurian-West, Xueyan Chen, Karen S. Kelly-Spratt, Christopher J. Kemp and James M. Roberts

Genes & Dev. 2006 20: 47-64
Access the most recent version at doi:10.1101/gad.1384406

A pathway in quiescent cells that controls p27^{Kip1} stability, subcellular localization, and tumor suppression

Arnaud Besson,[1] Mark Gurian-West,[1] Xueyan Chen,[1] Karen S. Kelly-Spratt,[2] Christopher J. Kemp,[2] and James M. Roberts[1,3]

[1]Howard Hughes Medical Institute, Division of Basic Sciences, [2]Division of Human Biology, Fred Hutchinson Cancer Research Center, Seattle, Washington 98109, USA

We have created two knock-in mouse models to study the mechanisms that regulate p27 in normal cells and cause misregulation of p27 in tumors: p27^{S10A}, in which Ser10 is mutated to Ala; and p27$^{CK^-}$, in which point mutations abrogate the ability of p27 to bind cyclins and CDKs. These two mutant alleles identify steps in a pathway that controls the proteasomal degradation of p27 uniquely in quiescent cells: Dephosphorylation of p27 on Ser10 inhibits p27 nuclear export and promotes its assembly into cyclin–CDK complexes, which is, in turn, necessary for p27 turnover. We further show that Ras-dependent lung tumorigenesis is associated with increased phosphorylation on Ser10 and cytoplasmic mislocalization of p27. Indeed, we find that p27^{S10A} is refractory to Ras-induced cytoplasmic translocation and that p27^{S10A} mice are tumor resistant. Thus, phosphorylation of p27 on Ser10 is an important event in the regulation of the tumor suppressor function of p27.

[*Keywords*: p27^{Kip1}; cyclin; CDK; tumor suppressor; tumorigenesis; Ras; lung cancer]

Supplemental material is available at http://www.genesdev.org.

Received October 14, 2005; revised version accepted November 11, 2005.

The transitions from one phase of the cell cycle to the next are driven by the activities of various cyclin/cyclin-dependent kinase (CDK) complexes (Sherr and Roberts 2004). One level of regulation of cyclin–CDK complexes is provided by cyclin–CDK inhibitors (CKIs), which modulate their activity (Sherr and Roberts 2001). The CKI p27^{Kip1} (p27) regulates the transition from G0, through G1, into S phase (Nourse et al. 1994; Polyak et al. 1994a,b; Toyoshima and Hunter 1994; Coats et al. 1996). The importance of p27 as a regulator of cell proliferation is illustrated by the phenotype of the *p27*-null mice, which display a marked increase in body size and multiorgan hyperplasia (Fero et al. 1996; Kiyokawa et al. 1996; Nakayama et al. 1996). Moreover, p27 is also a tumor suppressor in mice, as animals lacking p27 are predisposed to both spontaneous and induced tumorigenesis (Fero et al. 1996, 1998; Kiyokawa et al. 1996; Nakayama et al. 1996). p27 is haploinsufficient for tumor suppression, and loss of a single *p27* allele is sufficient to increase tumor incidence (Fero et al. 1998). p27 may also act as a tumor suppressor in humans, as decreased expression of nuclear p27 is commonly observed in various human cancers and is a significant prognostic marker for clinical outcome (Slingerland and Pagano 2000; Philipp-Staheli et al. 2001).

p27 protein levels are elevated in quiescent cells and decrease following mitogen stimulation and entry into G1 (Coats et al. 1996). p27 levels can be affected by transcriptional and translational pathways, but the major mechanisms for p27 regulation are thought to be post-translational proteolytic degradation (Pagano et al. 1995; Hengst and Reed 1996). Best understood is the proteolytic pathway that causes p27 degradation in late G1- and S-phase cells. Cdk2 first becomes active in late G1 and phosphorylates p27 on Thr187. This creates a recognition site for the Skp2–SCF E3 ubiquitin ligase, which ubiquitinates p27, thereby promoting its degradation by the proteasome (Sheaff et al. 1997; Vlach et al. 1997; Carrano et al. 1999; Montagnoli et al. 1999; Sutterluty et al. 1999; Tsvetkov et al. 1999). In addition, a stable interaction with cyclin–CDK complexes is important for p27 turnover. Thus, a p27$^{CK^-}$ mutant that cannot bind to cyclins and CDKs was still a substrate for phosphorylation on Thr187, but was not efficiently degraded (Vlach et al. 1997; Montagnoli et al. 1999). Supporting this idea, others have found a noncatalytic requirement for cyclin A–CDK2 complexes for p27 turnover (Zhu et al. 2004).

However, analysis of a p27^{T187A} knock-in mouse model revealed that this phosphorylation-resistant form

[3]**Corresponding author.**
E-MAIL jroberts@fhcrc.org; FAX (206) 667-6877.
Article and publication are at http://www.genesdev.org/cgi/doi/10.1101/gad.1384406.

of p27 was stabilized in S phase but was still degraded normally during G0 and G1, suggesting that other proteolytic pathways must exist (Malek et al. 2001). In fact, a second ubiquitin–proteasome pathway was recently described that causes the degradation of p27 in the cytoplasm during the G1 phase, mediated by the KPC1 and KPC2 E3 ubiquitin ligases (Kamura et al. 2004). CRM1-mediated nuclear export of p27 was necessary for KPC1–KPC2-mediated degradation, but it remains unknown whether a direct modification of p27, such as phosphorylation, is also required (Kamura et al. 2004). Moreover, it is unlikely that all p27 translocates into the cytosol in G1 cells (Rodier et al. 2001; Boehm et al. 2002; Ishida et al. 2002; Connor et al. 2003; McAllister et al. 2003; Kamura et al. 2004; Shin et al. 2005). Indeed, when p27 is confined to the nucleus either by pharmacological or genetic inhibition of its nuclear export, its stability decreases (Rodier et al. 2001). It is therefore probable that another turnover pathway acts during G1 in the nucleus. Whether it involves a Skp2-containing ubiquitin ligase that functions independently of Thr187 phosphorylation remains to be clarified (Malek et al. 2001).

The main phosphorylation site on p27 is Ser10, which has been found to regulate both its subcellular localization and stability (Ishida et al. 2000; Rodier et al. 2001). Phosphorylation at this site, or mutation of Ser10 to a phospho-mimetic residue (Asp or Glu), correlates with increased stability of p27, which is consistent with this being a modification primarily detected in nondividing cells (Ishida et al. 2000; Rodier et al. 2001; Boehm et al. 2002; Deng et al. 2004). The mechanism by which Ser10 phosphorylation stabilizes p27 in the G0 nucleus is not understood.

Although Ser10 phosphorylation is associated with p27 stabilization in quiescent cells, it has also been linked to p27 degradation in G1. Several groups reported that Ser10 phosphorylation of p27 was required for its export from the nucleus, possibly by mediating the binding of p27 to the exportin CRM1 (Rodier et al. 2001; Boehm et al. 2002; Ishida et al. 2002; Connor et al. 2003; McAllister et al. 2003; Shin et al. 2005). This may trigger p27 degradation in the cytoplasm of G1 cells, possibly by the KPC pathway. Several kinases are capable of phosphorylating p27 on Ser10: Mirk/dyrk1B phosphorylates and stabilizes p27 in quiescent cells (Deng et al. 2004), while hKIS phosphorylates this site at the G0–G1 transition following mitogen stimulation, and this is accompanied by translocation of p27 in the cytoplasm (Boehm et al. 2002). Other kinases, such as PKB/Akt and ERK2, were also reported to phosphorylate p27 on Ser10, at least in vitro (Ishida et al. 2000; Fujita et al. 2002).

The regulation of p27 stability and subcellular localization, which are critical for the control of p27 function, are complex phenomena modulated by phosphorylation and protein–protein interactions. In order to dissect the importance of these events in the regulation of p27 stability, localization, and function in vivo, both in physiological and pathological settings, we constructed knock-in mice harboring specific point mutations in the p27 gene. In the experiments described below, we focused on the unexpected interactions between two pathways that have been proposed to regulate p27 stability: its phosphorylation on Ser10 and its assembly into complexes with cyclins and CDKs. In quiescent cells, phosphorylation of p27 on Ser10 regulated its subcellular localization and its association with cyclin–CDK complexes, and this was critical for controlling p27 stability. Not only do we show that this constitutes a new turnover pathway for p27 that is uniquely active in quiescent cells but also that it represents a key mechanism for regulating the tumor suppressor function of p27.

Results

Generation of $p27^{S10A}$ and $p27^{CK^-}$ mice

To investigate the pathways that control p27 turnover, we engineered knock-in mice in which the *p27* gene was mutated at specific sites (Fig. 1A): In one strain, the $p27^{S10A}$ allele carried a mutation of Ser10, the main phosphorylation site on p27, to Ala (Ishida et al. 2000); in the other strain, the $p27^{CK^-}$ allele carried the mutations Arg30 to Ala and Leu32 to Ala in the cyclin-binding domain of p27, and Phe62 to Ala and Phe64 to Ala in the CDK-binding domain of p27. The $p27^{CK^-}$ mutation has previously been reported to abolish p27 binding to cyclins and CDKs (Vlach et al. 1997), and this was confirmed by us (see below). Precise replacement of the endogenous *p27* gene with the mutant alleles was confirmed by Southern blot (data not shown), genomic PCR (Fig. 1B), and DNA sequencing (data not shown). The progeny from $p27^{+/S10A} \times p27^{+/S10A}$ or $p27^{+/CK^-} \times p27^{+/CK}$ crosses were recovered with approximately the expected Mendelian ratios (Table 1). Below, we describe how mutation of either Ser10 or the cyclin–CDK-binding domain affects p27 function and regulation both in vivo and in cell culture, and then consider how these elements interact with each other to control p27 stability during the cell cycle.

The $p27^{CK^-}$ mutation

Mice lacking p27 have an increased growth rate and mature body size because of the occurrence of extra cell divisions in essentially all lineages, presumably a consequence of the lack of cyclin–CDK regulation by p27 (Fero et al. 1996; Kiyokawa et al. 1996; Nakayama et al. 1996). This is supported by the phenotype of the $p27^{CK^-}$ mice, which were similarly affected. We weighed cohorts of 30 animals per genotype weekly for 3 mo after weaning. Mice homozygous for $p27^{CK^-}$ were larger than their wild-type littermates, and $p27^{+/CK^-}$ had an intermediate phenotype (Fig. 1C, upper panels). Moreover, certain organs such as the spleen and thymus are differentially enlarged in p27-null mice, and those organs were also disproportionately larger in the $p27^{CK^-}$ background (Fig. 1D).

We confirmed that the $p27^{CK^-}$ protein did not associate with cyclins or CDKs. The presence of p27 bound to cyclins A, E1, or D1 was determined by immunoprecipi-

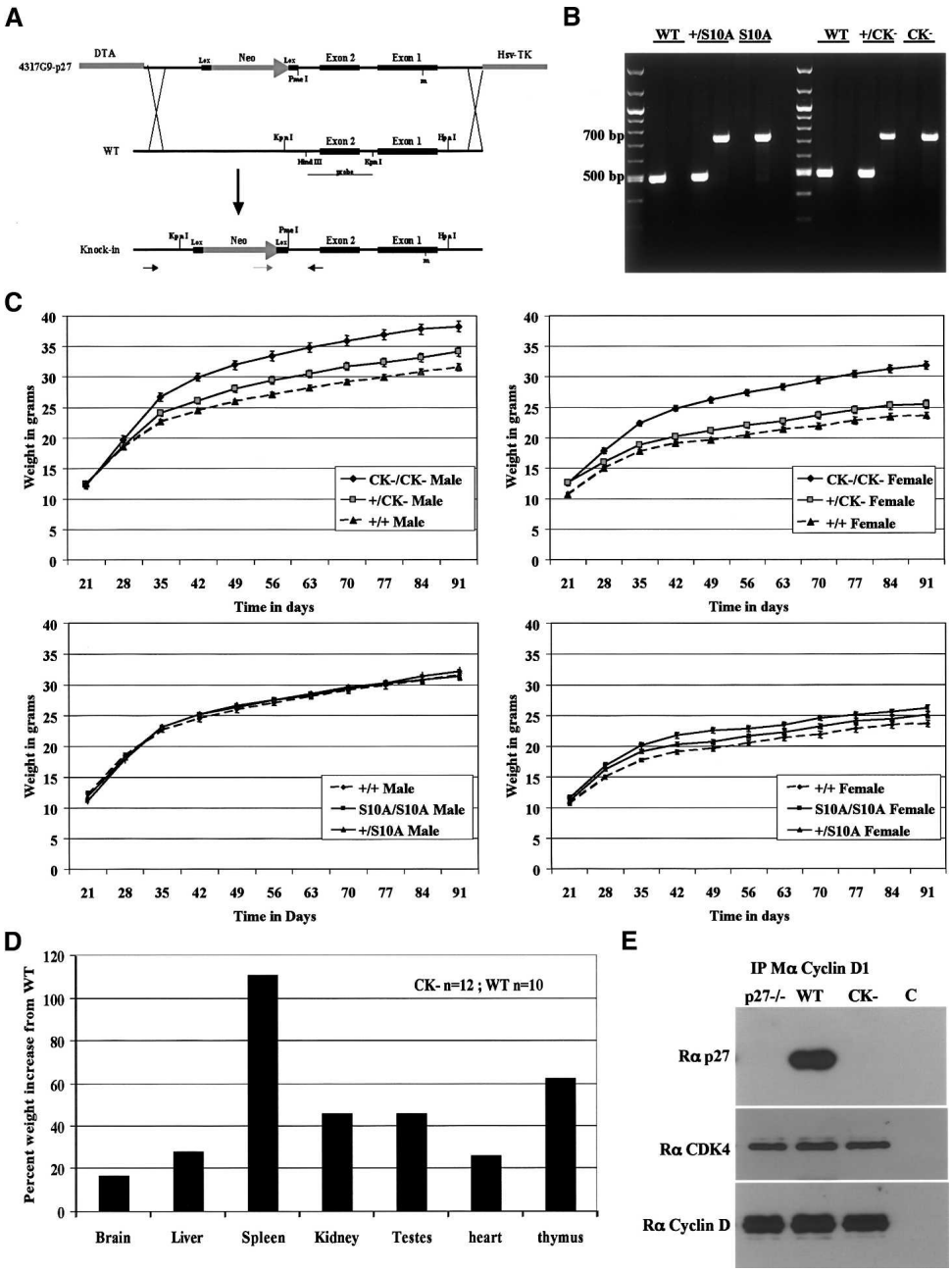

Figure 1. Construction of p27 mutant mice. (*A*) Targeting strategy for generating p27 knock-in mice. Schematic of the targeting construct used to replace the wild-type p27 genomic region with the $p27^{S10A}$ or $p27^{CK^-}$ alleles. The Southern probe as well as the PCR primers used for screening recombinant ES cells and genotyping transgenic mice are indicated. (*B*) Genotyping PCR. Using the primers shown in *A*, the wild-type allele gives a PCR product of ~500 bp and the recombinant allele (either $p27^{S10A}$ or $p27^{CK^-}$) a 700-bp product. (*C*) Size increase of the $p27^{CK^-/CK^-}$ mice. Thirty animals per genotype were weighed weekly from weaning to 3 mo of age. Both male and female $p27^{CK^-/CK^-}$ mice are larger than their wild-type counterparts. The size of $p27^{S10A/S10A}$ mice was not significantly affected, although females were slightly larger. (*D*) Percent increases in the mean weight of individual organs from 12 $p27^{CK^-/CK^-}$ males compared with that of 10 wild-type mice. (*E*) $p27^{CK^-}$ does not interact with cyclin D1. Cyclin D1 was immunoprecipitated from the indicated primary MEF extracts. Immunoprecipitates were resolved on SDS-PAGE and the membrane was probed for p27 (C19), stripped, and reprobed successively for CDK4 and cyclin D. The control lane (C) refers to an IP of wild-type extract with an irrelevant antibody.

tation (IP) from primary mouse embryonic fibroblast (MEF) extracts. Whereas wild-type p27 associated with all three cyclins, the $p27^{CK^-}$ protein was associated with none (Figs. 1E, 5D–F; Supplementary Fig. 5). Thus, both phenotypic and molecular observations confirm that the $p27^{CK^-}$ mutation prevents the interaction of p27 with cyclins and CDKs. We are continuing to characterize the phenotype of $p27^{CK^-}$ mice in order to address whether

Table 1. *Ratios of $p27^{+/CK^-}$ × $p27^{+/CK^-}$ and $p27^{+/S10A}$ × $p27^{+/S10A}$ progeny*

+/S10A × +/S10A	Genotype	+/+	+/S10A	S10A/S10A
Number of animals	314	73	163	78
Percentage	100%	23.2%	51.9%	24.8%
+/CK⁻ × +/CK⁻	Genotype	+/+	+/CK⁻	CK⁻/CK⁻
Number of animals	327	96	153	78
Percentage	100%	29.3%	46.8%	23.9%

there are cyclin–CDK-independent functions of p27 (A. Besson and J.M. Roberts, in prep.).

We next examined the effect of the $p27^{CK^-}$ mutation on the abundance of the p27 protein in vivo. In all tissues tested (spleen, uterus, brain, liver, thymus, and lung), $p27^{CK^-}$ levels were increased (Fig. 2A; data not shown). Similar results were obtained by immunohistochemistry, which revealed a stronger signal for $p27^{CK^-}$ than wild-type p27 in the brain (Supplementary Fig. 1A). p27 levels in primary MEFs derived from wild-type and $p27^{CK^-}$ embryos were similar to those observed in tissues, with $p27^{CK^-}$ being elevated in all conditions (exponentially growing, serum starved, or confluent) (Fig. 2C).

To further explore the effect of the $p27^{CK^-}$ mutation on p27 abundance, we monitored primary MEFs following serum stimulation over a 24-h time course both for p27 levels (Fig. 2D) and progression through the cell cycle by flow cytometry (Fig. 2E). As previously reported, wild-type p27 levels were elevated in serum-starved cells, progressively decreased during G1 (between 3 h and 15 h), and remained low in S phase (between 18 h and 24 h). In contrast, $p27^{CK^-}$ protein levels were strikingly different from wild-type p27. As expected, the relative abundance of the $p27^{CK^-}$ protein was increased in S-phase cells, consistent with the requirement for phosphorylation of p27 by cyclin E–CDK2 and binding to cyclin–CDK for ubiquitination by the SCF-Skp2 E3 ligase (Sheaff et al. 1997; Vlach et al. 1997; Montagnoli et al. 1999; Zhu et al. 2004). Surprisingly, the $p27^{CK^-}$ protein was also elevated in quiescence, suggesting that cyclin–CDK–p27 heterotrimer assembly also sets the level of p27 in nondividing cells. The $p27^{CK^-}$ protein behaved similarly to wild-type p27 only during entry into G1 following serum stimulation, where both proteins were effectively down-regulated (Fig. 2D). Thus, p27 regulation during G1 was independent of its binding to cyclins and CDKs and therefore proceeded by a pathway that was distinct from those that operated in quiescence and S phases.

We directly tested whether the $p27^{CK^-}$ mutation affected p27 steady-state abundance by changing its rate of degradation. The rate of p27 turnover was measured in exponentially growing (Fig. 3A), serum-starved (Fig. 3B), G1-phase (Fig. 3C), and S-phase (Fig. 3D) primary MEFs using cycloheximide to block protein synthesis. The graph in Figure 3E represents the means and standard deviations for p27 half-lives obtained in multiple experiments at each phase of the cell cycle. In every case, the effect of the $p27^{CK^-}$ mutation on p27 steady-state protein abundance could be explained by its effect on p27 turnover. The $p27^{CK^-}$ protein was more stable than wild-type p27 in exponentially growing cells, in S-phase cells, and in quiescent cells (Fig. 3). Importantly, the rate of $p27^{CK^-}$ degradation was significantly increased during G1 compared with other phases of the cell cycle (Fig. 3C,E), with the small difference between it and wild-type p27 probably reflecting the fact that not all cells entered the cell cycle following serum stimulation and that this was therefore only an enriched population for G1 cells (Fig. 3E). We concluded that the formation of heterotrimeric p27–cyclin–CDK complexes is required for p27 degradation both in quiescent cells and during S phase.

The $p27^{S10A}$ mutation

In confirmation of recent reports, we observed that the abundance of the $p27^{S10A}$ protein was decreased in quiescent cells compared with wild-type p27, both in vivo and in vitro (Deng et al. 2004; Kotake et al. 2005). $p27^{S10A}$ protein levels were decreased in extracts from all tissues examined (Fig. 2A,B), and this was consistent with p27 immunohistochemistry in the brain of $p27^{S10A}$ mice (Supplementary Fig. 1B). As expected, no signal was detected when extracts from the brain or MEFs from $p27^{S10A}$ mice were probed with a phospho-Ser10 p27-specific antibody, while both wild-type p27 and $p27^{CK^-}$ displayed abundant Ser10 phosphorylation (Fig. 2B,C). Similarly to what was observed in tissues, the $p27^{S10A}$ protein was decreased in abundance relative to wild-type p27 in primary MEFs independently of culture conditions (Fig. 2C).

Analyses of synchronized MEFs demonstrated that the *$p27^{S10A}$* mutation specifically affected p27 abundance and stability in quiescent cells. $p27^{S10A}$ protein levels were low in quiescent MEFs, and in response to serum stimulation they were rapidly down-regulated to lower levels than wild-type p27 in G1 and S phases (Fig. 2D). No significant difference in cell cycle distribution was observed by flow cytometric analyses between wild-type p27, $p27^{CK^-}$, and $p27^{S10A}$ MEFs following serum stimulation (Fig. 2E). To determine whether the difference in abundance of $p27^{S10A}$ was due to altered turnover rate of the protein, the half-life of $p27^{S10A}$ was determined in the various phases of the cell cycle (Fig. 3). In MEFs serum starved for 72 h, $p27^{S10A}$ had a considerably shorter half-life (~4.5 h) than wild-type p27 (~8 h), indicating that phosphorylation of p27 on Ser10 normally stabilizes p27 in quiescent cells (Fig. 3B,E). On the other hand, the S10A mutation had relatively little effect on p27 stability in G1 or S phases (Fig. 3C–E). To confirm that the lack of Ser10 phosphorylation was, indeed, responsible for the instability of $p27^{S10A}$ in quiescent cells, a $p27^{S10E}$ mutant, in which Ser10 is replaced by the phospho-mimetic amino acid Glu, was expressed in p27-null MEFs. In quiescent cells, $p27^{S10E}$ was very stable following cycloheximide treatment compared with wild-type p27 or $p27^{S10A}$ (Fig. 4A). We also found that p27 was degraded via a proteasome-dependent pathway in quiescent cells, as addition of the proteasome inhibitor MG132 in con-

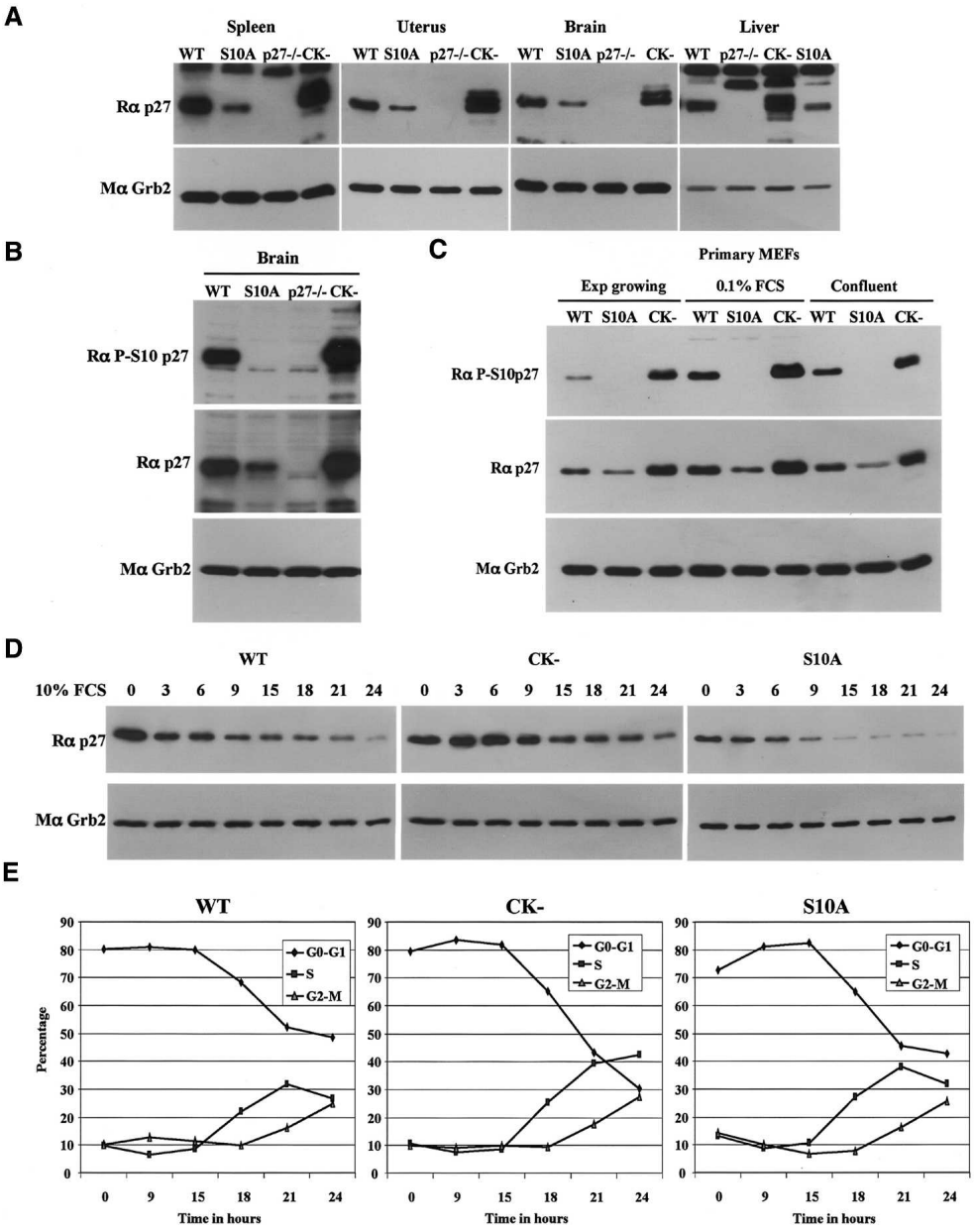

Figure 2. Opposite effects of the $p27^{CK^-}$ and $p27^{S10A}$ mutations on p27 levels and on p27 degradation following growth stimulation. (*A*) Tissue expression of p27 in $p27^{+/+}$ (WT), $p27^{S10A}$ (S10A), $p27^{-/-}$, and $p27^{CK^-}$ (CK^-) mice. Equal amounts of tissue extracts (spleen, brain, uterus, liver) were probed successively with a polyclonal p27 antibody (C19) and with a monoclonal anti-Grb2 antibody to evaluate protein loading. (*B*) Lack of Ser10 phosphorylation of the $p27^{S10A}$ mutant. Brain extracts were probed successively with a phospho-Ser10 p27-specific antibody, and for p27 and Grb2 (loading control). (*C*) $p27^{S10A}$ and $p27^{CK^-}$ levels in primary MEFs in different culture conditions. MEFs were either exponentially growing (Exp growing), serum starved for 72 h (0.1% FCS), or kept confluent for 24 h (Confluent). The membrane was probed as in *B*. (*D*) $p27^{S10A}$ and $p27^{CK^-}$ have oppositely altered kinetics of degradation following serum stimulation. Wild-type, $p27^{S10A}$, and $p27^{CK^-}$ primary MEFs were serum starved for 72 h and replated in the presence of 10% serum. Membranes were probed as in *A*. (*E*) Flow cytometric analyses of the cell cycle of wild-type, $p27^{S10A}$, and $p27^{CK^-}$ primary MEFs. Parallel cell cultures as in *D* were treated similarly and collected for flow cytometry.

junction with cycloheximide efficiently blocked wild-type p27, $p27^{CK^-}$, and $p27^{S10A}$ turnover (Fig. 4B).

Mechanism of stabilization of $p27^{CK^-}$

Our data indicate that p27 turnover in G0 requires binding to cyclin/CDK complexes. However, which cyclins and/or CDKs are involved and whether CDK activity is required are unclear. To determine the importance of a direct interaction with cyclin or CDK or both proteins in p27 turnover in G0, we measured the half-lives of $p27^{C^-}$ (Arg30 to Ala and Leu32 to Ala) and $p27^{K^-}$ (Phe62 to Ala and Phe64 to Ala). The interaction with cyclin appeared critical for turnover in quiescent cells, as $p27^{C^-}$ had a

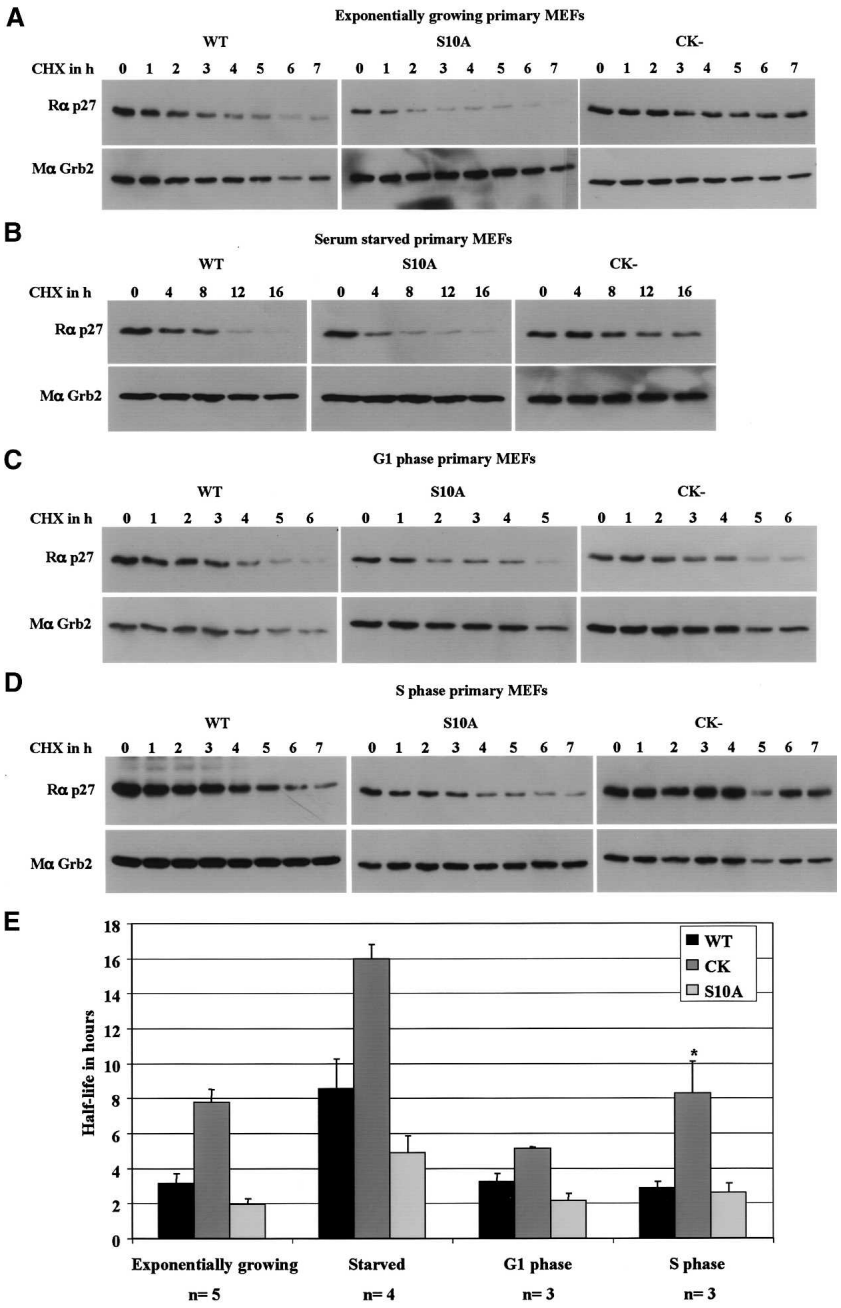

Figure 3. $p27^{S10A}$ is unstable in quiescent cells, while $p27^{CK^-}$ is stabilized in G0 and S phases. p27 half-life determination in exponentially growing (*A*), serum-starved for 72 h (*B*), G1-phase (*C*), and S-phase (*D*) wild-type (WT), $p27^{S10A}$ (S10A), and $p27^{CK^-}$ (CK^-) primary MEFs. (*A–D*) Primary MEFs in the indicated culture conditions were treated with 25 μg/mL cycloheximide (CHX) and collected at the indicated time. A polyclonal p27 antibody (C19), and a monoclonal Grb2 (loading control) were used for immunoblotting. (*E*) Summary of p27 half-life data from several experiments: exponentially growing ($n = 5$), serum starved ($n = 4$), G1 phase ($n = 3$), and S phase ($n = 3$). For each experiment, p27 immunoblots were quantified and the amount of p27 expressed as percent of p27 remaining from time zero. Half-lives were determined from the individual graphs by drawing a "best fit" curve for each cell type and condition. (*) Note that the $p27^{CK^-}$ half-life in S phase is underestimated in the graph as essentially no turnover occurred during the time frame in one experiment (i.e., $T½ \gg 7$ h), and this experiment therefore could not be included in the calculation of half-life.

half-life similar to that of $p27^{CK^-}$; however, the interaction with CDK may also be important since the half-life of $p27^{K^-}$ was intermediate between wild-type p27 and $p27^{C^-}$ (Fig. 4C). This was consistent with previous data showing that the cyclin-binding domain is more important for the stable assembly of the p27–cyclin–CDK complex than is the CDK-binding domain (Vlach et al. 1997), and was also in agreement with a study on the requirements for p27 ubiquitination in vitro (Ungermannova et al. 2005). Pharmacological CDK inhibitors, roscovitine or olomoucine, had no significant effect on p27 half-life in serum-starved wild-type or $p27^{S10A}$ primary MEFs (Supplementary Fig. 2), indicating that CDK activity was not required for p27 turnover during quiescence. Next we monitored p27 half-life in MEFs lacking specific cyclins or CDKs (cyclin $D1^{-/-}$, cyclin $D1/D2^{-/-}$, cyclin $E1/E2^{-/-}$, $CDK2^{-/-}$, and $CDK4^{-/-}$). The absence of one type of cyclin or CDK did not significantly affect p27 half-life in G0 (Supplementary Fig. 3). Therefore, the cyclin/CDK complexes that are present in quiescent cells may be functionally interchangeable with respect to promoting p27 turnover.

One of the amino acids mutated in $p27^{CK^-}$, Leu32, is part of a putative nuclear export signal in p27 (between amino acids 32 and 45) and has been proposed to mediate p27's interaction with CRM1 (Connor et al. 2003). How-

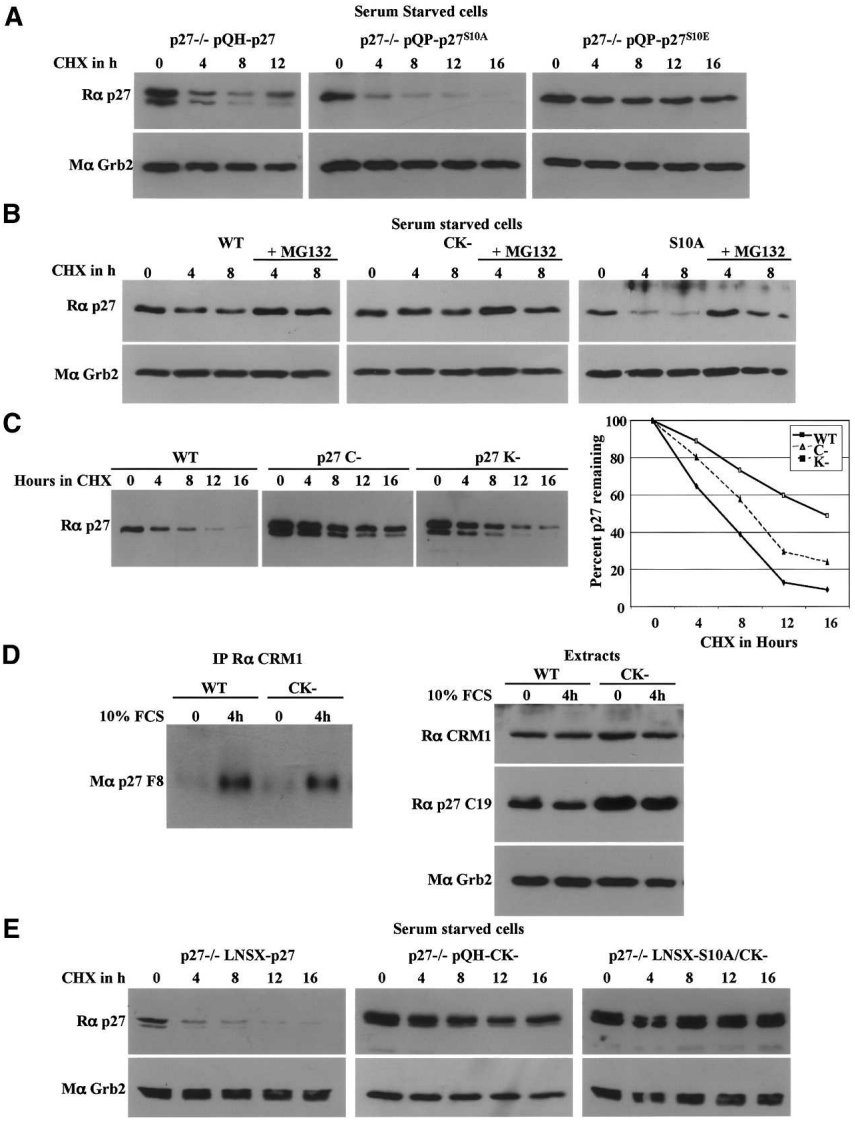

Figure 4. The instability of $p27^{S10A}$ depends on its ability to interact with cyclin–CDK complexes. (*A*) A Ser10-phosphomimetic mutant ($p27^{S10E}$) is stable in quiescent cells. p27-null immortalized MEFs were retrovirally infected with either wild-type p27 ($p27^{-/-}$pQH-p27), $p27^{S10A}$ ($p27^{-/-}$pQP-$p27^{S10A}$), or $p27^{S10E}$ ($p27^{-/-}$pQP-$p27^{S10E}$). After selection of infected MEFs, cells were serum starved, treated with CHX, and processed as described in Figure 3. (*B*) p27 degradation is proteasome-dependent in quiescent cells. Wild type (WT), $p27^{S10A}$ (S10A), and $p27^{CK^-}$ (CK^-) primary MEFs were serum starved for 72 h and treated with 25 µg/mL CHX or with both CHX and 10 µM MG132 for the indicated time. Samples were processed as in Figure 3. (*C*) Cyclin interaction is critical for p27 turnover in G0. The half-lives of wild-type p27, $p27^{C^-}$ ($p27^{-/-}$pQP-$p27^{C^-}$), and $p27^{K^-}$ ($p27^{-/-}$pQP-$p27^{K^-}$) were determined as in *A*. (*D*) $p27^{CK^-}$ can still interact with CRM1. CRM1 was immunoprecipitated from extracts prepared from primary wild-type or $p27^{CK^-}$ MEFs either serum starved for 72 h, or starved and stimulated for 4 h with 10% serum. Immunoprecipitates were resolved on SDS-PAGE and probed for p27. A fraction of the extracts was used for Western blotting to determine the amounts of CRM1, p27, and Grb2 (loading control) present in these cells. (*E*) Stabilization of a $p27^{S10A}$ mutant that cannot bind cyclins and CDKs ($p27^{S10A/CK^-}$) in quiescent cells. p27-null MEFs were retrovirally infected with either wild-type p27 ($p27^{-/-}$LNSX-p27), $p27^{CK^-}$ ($p27^{-/-}$pQH-CK^-), or $p27^{S10A/CK^-}$ ($p27^{-/-}$LNSX-S10A/CK^-), and treated as in *A*.

ever, we found that endogenous $p27^{CK^-}$ could be coimmunoprecipitated with endogenous CRM1, similarly to wild-type p27 (Fig. 4D). This ruled out the possibility that the $p27^{CK^-}$ mutation increased p27 stability due to a defect in CRM1-mediated export. The increased stability of the $p27^{K^-}$ protein, which is mutated outside of the proposed CRM1-binding domain, also indicated that the affected turnover pathway did not involve CRM1.

A pathway for p27 turnover in quiescent cells

Phosphorylation of p27 on Ser10 and the ability of p27 to interact with cyclins and CDKs both regulate p27 stability in quiescent cells. To determine if these events were part of a single pathway, we tested how the conjunction of the S10A and CK^- mutations affected p27 stability. We found that the $p27^{S10A/CK^-}$ double mutant was as stable as the $p27^{CK^-}$ mutant in quiescent (Fig. 4E) or exponentially growing cells (Supplementary Fig. 4), suggesting that cyclin–CDK assembly functions downstream of, or coincidentally with, Ser10 phosphorylation to control p27 stability.

An attractive hypothesis to explain the above result is that Ser10 phosphorylation may determine the rate of p27 turnover by inhibiting the ability of p27 to associate with cyclins and CDKs. Indeed, we found that the $p27^{S10A}$ mutation had a dramatic effect on p27 assembly into cyclin–CDK complexes. We performed IPs using a monoclonal p27 antibody (F8) that recognizes free p27, but not p27 bound to cyclin–CDK complexes (see below). When this antibody was used to immunoprecipitate p27 in serum-starved or exponentially growing primary MEF extracts (Fig. 5A,B, respectively), hardly any $p27^{S10A}$ was detected, while wild-type p27 and $p27^{CK^-}$ were readily detected, consistent with the fact that the latter cannot bind cyclins and CDKs. In addition, no cyclin D was detected in these IPs (Fig. 5A,C). To rule out the possibility that the S10A mutation disrupted the epitope recognized by this antibody, we used $p27^{-/-}$ MEFs retrovi-

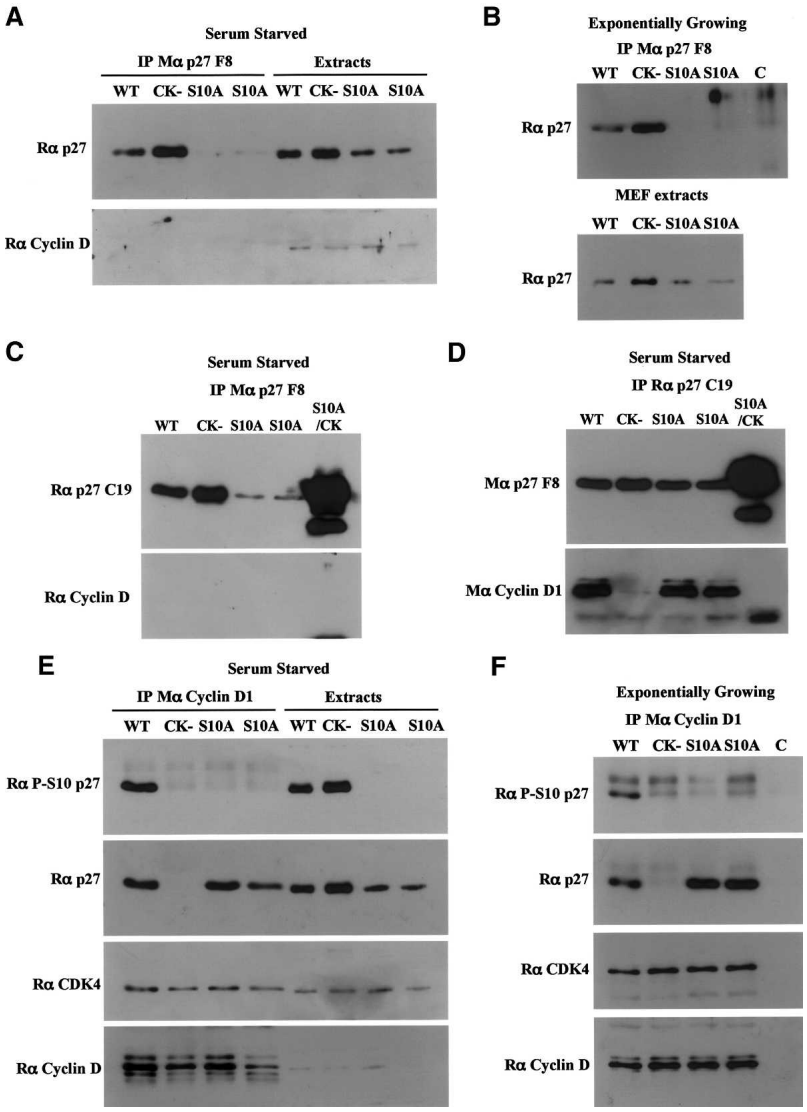

Figure 5. Most $p27^{S10A}$ is bound to cyclin–CDK complexes. IPs in primary MEF protein extracts. (*A*,*B*) IP with a monoclonal p27 antibody (p27 F8) that immunoprecipitates only free p27 in serum-starved (*A*) or exponentially growing (*B*) cells. The amounts of p27 present in the cell extracts used for IP are also indicated. Immunoprecipitates were resolved on SDS-PAGE, and membranes were probed with a polyclonal p27 antibody (C19). In *A*, the membrane was stripped and reprobed with a polyclonal antibody to cyclin D. (*C*) Same as *A*, except that an additional extract from $p27^{-/-}$ cells expressing a $p27^{S10A/CK^-}$ mutant was used for IP. (*D*) Same as *C* with IPs performed with a polyclonal p27 antibody (C19) that immunoprecipitates all forms of p27. (*E*,*F*) IPs with a monoclonal cyclin D1 antibody in serum-starved (*E*) or exponentially growing (*F*) primary MEFs. Membranes were probed successively with polyclonal antibodies to phospho-Ser10 p27, p27, CDK4, and cyclin D. For *F*, the cell extracts used were the same as in *B*. In *B* and *F*, the control lane (C) corresponds to an IP of wild-type extract performed with an irrelevant antibody.

rally infected with the $p27^{S10A/CK^-}$ double mutant. This mutant was immunoprecipitated very efficiently by the p27 F8 antibody, while very little $p27^{S10A}$ could be detected (Fig. 5C). In contrast, coimmunoprecipitation of cyclin D1 with either wild-type p27 or $p27^{S10A}$ was readily detected with a polyclonal anti-p27 antibody (Fig. 5D), while no cyclin D1 could be detected in association with $p27^{CK^-}$ or $p27^{S10A/CK^-}$. Thus, most $p27^{S10A}$ protein is bound to cyclin–CDK complexes, whereas the wild-type p27 protein is found in both the bound and free compartments.

In further support of an effect of the $p27^{S10A}$ mutation on p27's assembly into cyclin–CDK complexes, coimmunoprecipitation experiments were performed to measure the amount of p27 associated with various cyclins. In serum-starved primary MEFs, the amount of $p27^{S10A}$ coimmunoprecipitated with cyclin D1 was similar to the amount of wild-type p27 associated with cyclin D1, despite the fact that the total amount of $p27^{S10A}$ in the cell was reduced compared with wild-type p27 (Fig. 5E). Similar results were obtained in exponentially growing MEFs (Fig. 5F). Likewise, Cyclin A and Cyclin E coimmunoprecipitations yielded similar or higher amounts of $p27^{S10A}$ compared with wild-type p27 (Supplementary Fig. 5), despite the lower overall abundance of $p27^{S10A}$.

The increased ability of the $p27^{S10A}$ protein to associate with cyclins and CDKs was also supported by the phenotype of the knock-in mice. $p27^{S10A/S10A}$ homozygous mice expressed the p27 protein at a level similar to mice heterozygous for p27 ($p27^{+/-}$; i.e., 50% of normal wild-type levels). However, whereas $p27^{+/-}$ mice showed an increased body size and generalized organomegaly (Fero et al. 1996), the $p27^{S10A/S10A}$ homozygous male mice were indistinguishable from wild-type mice in these respects, and the $p27^{S10A/S10A}$ homozygous females had an increased size of only borderline significance (Fig. 1C). Together, the molecular and phenotypic data show that the $p27^{S10A}$ mutation promotes the association of p27 with cyclin–CDK complexes, and suggest that Ser10 phosphorylation and heterotrimer assembly

operate in a single p27 turnover pathway in quiescent cells.

One possible explanation for these data is that Ser10 phosphorylation directly affects the binding of p27 to cyclins and CDKs or that it modulates its ability to inhibit cyclin/CDK complexes. To test this, the ability of recombinant p27, $p27^{S10A}$, and the phospho-mimetic mutant $p27^{S10E}$ to bind to and inhibit cyclin E–CDK2 in vitro was measured. We found that the amounts of recombinant p27, $p27^{S10A}$, and $p27^{S10E}$ bound to cyclin E–CDK2 were similar (Fig. 6A). Likewise, the Ki of these three forms of p27 for inhibition of recombinant cyclin E–CDK2 were almost indistinguishable (Fig. 6B), indicating that the abilities of these proteins to bind to and to inhibit cyclin E–CDK2 complexes in vitro were not substantially different from one another.

An alternative hypothesis to explain the sequestration of $p27^{S10A}$ into cyclin–CDK complexes was that Ser10 phosphorylation promoted p27 export to the cytoplasm, which would create a pool of unbound p27 by segregating it from its cyclin and CDK partners (Rodier et al. 2001; Boehm et al. 2002; Ishida et al. 2002; Connor et al. 2003). To address this, the subcellular localization of the $p27^{S10A}$ and wild-type p27 proteins in MEFs was compared. In these experiments we previously found it crucial to use p27-null MEFs as a control, because all available p27 antibodies detect a modest nonspecific background signal in the cytoplasm of fibroblasts (Besson et al. 2004b). Wild-type p27 MEFs contained a prominent nuclear pool of the p27 protein, and additionally a weak cytoplasmic signal that was reproducibly stronger than the background detected in the p27-null cells (Fig. 7; Supplementary Fig. 6; Besson et al. 2004b). $p27^{S10A}$ cells also contained a clear nuclear pool of p27 protein, but the cytoplasmic signal did not surpass the nonspecific background signal detected in the p27-null cells (Fig. 7; Supplementary Fig. 6). Nevertheless, since the overall amount of $p27^{S10A}$ was lower than the wild-type p27 protein, it was possible that some cytoplasmic $p27^{S10A}$ protein was below the limit of detection. To overcome this limitation, similar experiments were performed in the presence of the proteasome inhibitor MG132, so that if p27 were unstable in the cytoplasm, its abundance would be increased by proteasome inhibition, making it readily detectable. Indeed, in the presence of MG132, a clear pool of cytoplasmic p27 was visible in wild-type MEFs (Fig. 7; Supplementary Fig. 6). This pool was more abundant following serum stimulation, consistent with previous reports that p27 nuclear export is increased in proliferating cells (Rodier et al. 2001; Boehm et al. 2002; Connor et al. 2003; Shin et al. 2005). In contrast, although proteasome inhibition increased the abundance of nuclear $p27^{S10A}$, hardly any $p27^{S10A}$ could be detected in the cytoplasm (Fig. 7; Supplementary Fig. 6). Further evidence in support of the hypothesis that the $p27^{S10A}$ mutation alters the subcellular localization of the protein is provided below, as is evidence that misregulation of this pathway is critical during tumor progression. Thus, our results suggest that the increased association of $p27^{S10A}$ with cyclin–CDK complexes is a likely consequence of its sequestration in the nucleus.

Phosphorylation on Ser10 controls tumor suppression by p27

p27 is a dosage-dependent tumor suppressor (Fero et al. 1998). Since the $p27^{S10A/S10A}$ homozygous mouse ex-

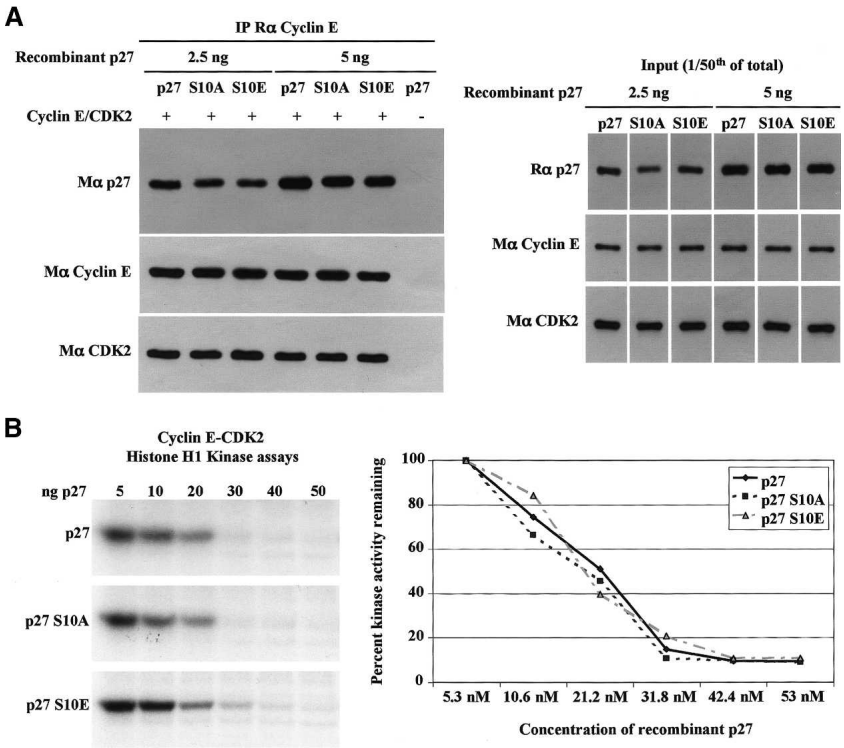

Figure 6. $p27^{S10A}$, $p27^{S10E}$, and wild-type p27 bind to and inhibit cyclin E–CDK2 complexes in vitro equivalently. (*A*) Recombinant wild-type p27, $p27^{S10A}$, and $p27^{S10E}$ bind cyclin E–CDK2 complexes with similar affinities. The indicated amounts of recombinant p27 proteins were incubated with cyclin E–CDK2 complexes expressed in SF21 cells. Cyclin E was then immunoprecipitated, and the amount of p27 coprecipitated was determined by Western blotting; amounts of cyclin E and CDK2 immunoprecipitated are also shown. The *right* panel shows the starting amounts of proteins used in the binding assay. (*B*) Recombinant wild-type p27, $p27^{S10A}$, and $p27^{S10E}$ have similar abilities to inhibit cyclin E–CDK2 complexes in in vitro histone H1 kinase assays. The graph indicates the percent of kinase activity remaining normalized to the control reaction, where there is no inhibition by p27.

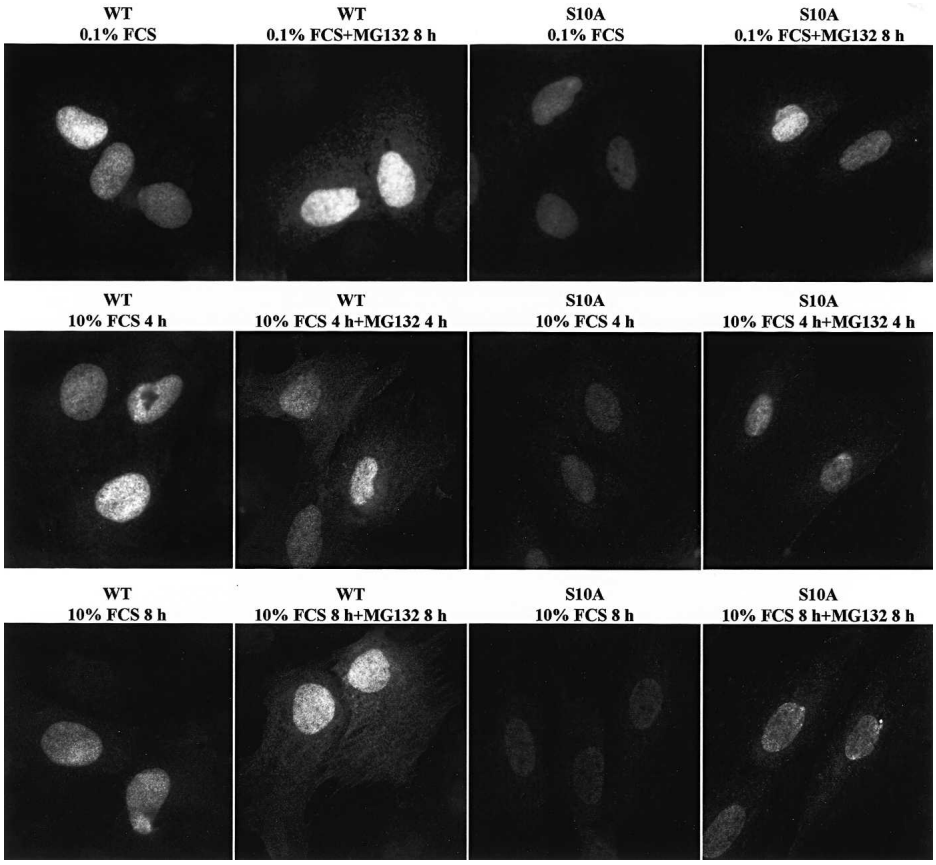

Figure 7. Nuclear sequestration of $p27^{S10A}$. Immunofluorescence with a monoclonal p27 antibody (clone 57; BD-Transduction Laboratories) in the presence or absence of 10 μM MG132 in wild-type and $p27^{S10A}$ MEFs either serum starved for 48 h (0.1% FCS), or starved and stimulated with 10% FCS for 4 h or 8 h. All images were taken with identical settings using a 100× lens, with the exposure time calculated on $p27^{-/-}$ MEFs processed identically so that the nonspecific staining of the antibody was not visible.

pressed reduced amounts of p27, it might have been predicted that it would demonstrate increased tumor susceptibility, similar to the $p27^{+/-}$ mouse. However, the $p27^{S10A}$ mutation increases its association with cyclin–CDK complexes, probably by enforcing the nuclear retention of p27, and thus may enhance the ability of p27 to inhibit cell proliferation. Therefore, the overall effect of the Ser10 pathway on tumor suppression was not easily predicted.

To address the importance of Ser10 phosphorylation in controlling tumor suppression by p27, we compared the susceptibility of wild-type, $p27^{+/-}$, $p27^{-/-}$, and $p27^{S10A/S10A}$ mice to urethane-induced tumorigenesis. In this model, mice develop primarily lung tumors that carry an activating mutation at codon 61 of the K-Ras oncogene (Barbin 2000; Meuwissen and Berns 2005). Loss of one allele of p27 was sufficient to significantly increase the number of lung tumors compared with wild-type animals, but the loss of both p27 alleles did not further increase tumor number (Fig. 8A). Even though $p27^{S10A}$ protein levels in the lungs were similar to the p27 levels found in the p27 heterozygous mice (Fig. 8B), $p27^{S10A/S10A}$ mice developed less tumors than all the other groups. Thus, despite equivalent levels of p27 protein expression, $p27^{S10A/S10A}$ mice were substantially less susceptible to lung tumor development than $p27^{+/-}$ animals (~6.7 tumors per animal compared with 12.6, respectively).

When lung tumors were scored according to their size, the number of small tumors (0–2 mm) mirrored the total number of tumors (Fig. 8C). However, the number of large tumors (2–4 mm) was directly proportional to the number of p27 alleles: $p27^{-/-}$ mice had more large tumors than $p27^{+/-}$ animals, and the latter had more large tumors than wild-type mice (Fig. 8D). These results suggested that the growth rate of tumors was related to the dosage of the p27 protein, with the absence of p27 allowing for faster growth. In contrast, $p27^{S10A/S10A}$ had a greatly reduced number of large tumors compared with $p27^{+/-}$, suggesting that tumors arising in the former had reduced growth rate (Fig. 8D). Figure 8E shows representative lungs from urethane-treated animals of each genotype. In sum, $p27^{S10A/S10A}$ mice were partially resistant to lung tumor development, and the growth rate of tumors arising in $p27^{S10A/S10A}$ animals was reduced.

Although our studies focused on lung tumorigenesis, urethane treatment for 20 wk resulted in pituitary adenomas and harderian gland tumors exclusively in the

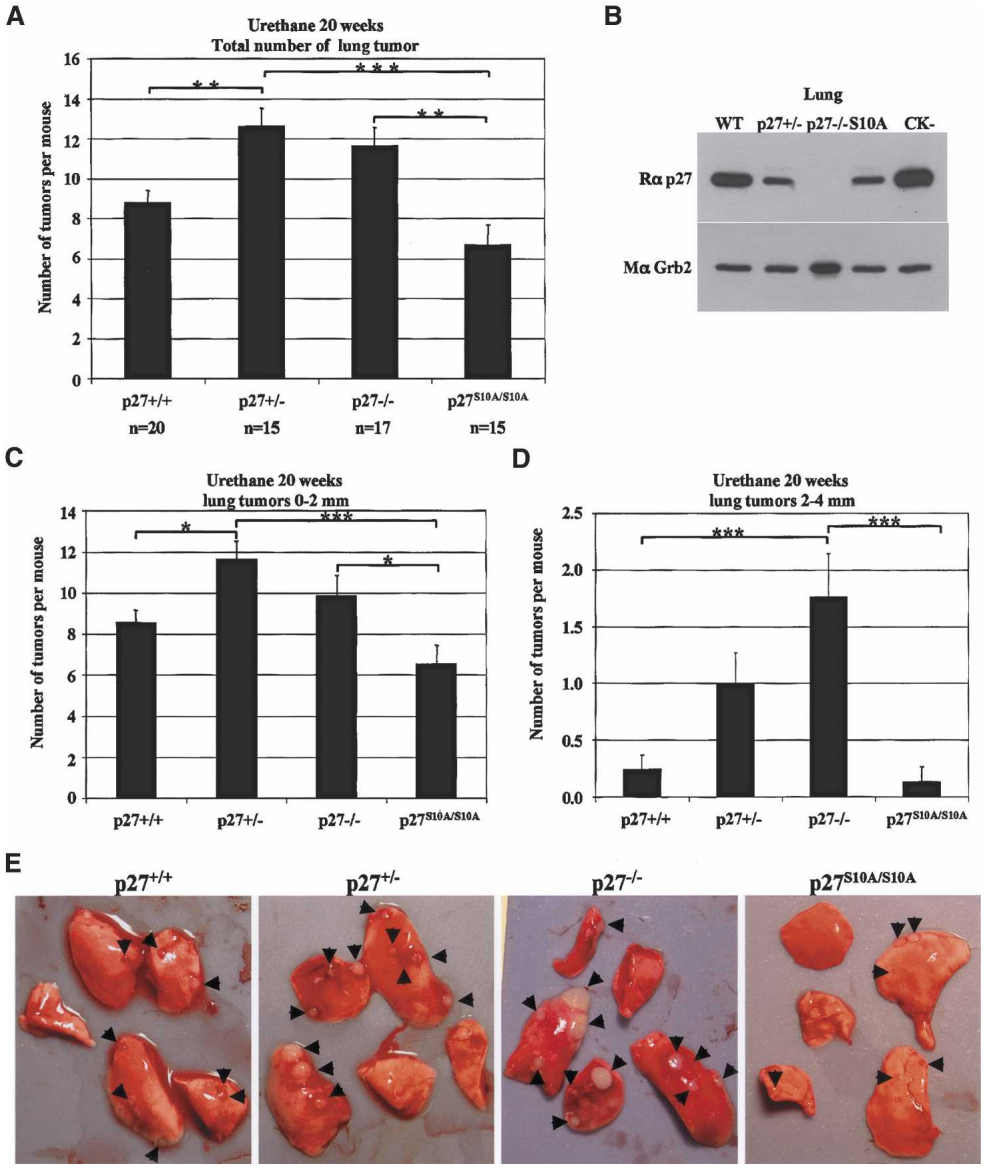

Figure 8. Decreased incidence and growth rate of urethane-induced lung tumors in $p27^{S10A}$ mice. (*A*) Total number of lung tumors in wild-type, $p27^{+/-}$, $p27^{-/-}$, and $p27^{S10A}$ mice 20 wk following a single dose of urethane. Lungs were dissected and macroscopic tumors were counted by visual inspection. The results were analyzed using a one-way analysis of variance with the Tukey-Kramer multiple comparison test. (***) $p < 0.001$; (**) $p < 0.01$; (*) $p < 0.05$. (*B*) $p27^{S10A}$ protein levels in the lung are similar to p27 levels in $p27^{+/-}$ mice. Lung extracts from wild-type (WT), $p27^{+/-}$, $p27^{-/-}$, $p27^{S10A/S10A}$ (S10A), and $p27^{CK^-}$/CK^- (CK^-) mice were resolved on SDS-PAGE, and the membrane was probed with a polyclonal p27 (C19) antibody, stripped, and reprobed with a monoclonal Grb2 antibody to evaluate protein loading. (*C*,*D*) Lung tumors were counted according to their size: small tumors (between 0 and 2 mm in diameter) (*C*), and large tumors (between 2 and 4 mm in diameter) (*D*). Statistical analyses were performed as in *A*. (*E*) Representative lungs for each mouse genotype following dissection. Tumors are indicated by arrows.

p27-null mice with a 100% penetrance (Table 2). Liver hemangiomas were observed in animals of all genotypes, with incidence increasing with the reduction of the number of p27 alleles; and the lowest incidence observed in $p27^{S10A/S10A}$ animals (Table 2). Uterine tumors were observed with increasing penetrance in $p27^{+/-}$ and $p27^{-/-}$ mice, but not in wild-type or $p27^{S10A/S10A}$ animals. Ovarian granulosa cell tumors were seen in all genotypes, but were more prominent in $p27^{-/-}$ mice (Table 2).

Histological analyses revealed that all tumors developing in the lungs, regardless of the genotype of the mice, were a mix of bronchioalveolar adenomas and papillary adenomas (Fig. 9A). Cytoplasmic localization of p27 is observed in many types of human cancers and is considered a negative factor for prognosis (Slingerland and Pagano 2000; Philipp-Staheli et al. 2001; Liang et al. 2002). In normal lung tissue, p27 was mostly localized in the nuclei; however; in the tumors from wild-type and $p27^{+/-}$ mice, p27 was largely excluded from the nuclei of

Table 2. *Reduced incidence of urethane-induced tumors in p27^{S10A} mice*

	$p27^{+/+}$	$p27^{+/-}$	$p27^{-/-}$	$p27^{S10A/S10A}$
Tumor type	Tumor incidence in % (number of cases/total number of individuals)			
Pituitary tumor	0 (0/20)	0 (0/16)	100 (17/17)	0 (0/15)
Harderian gland tumor	0 (0/20)	0 (0/16)	100 (17/17)	0 (0/15)
Uterine hyperplasia	0 (0/8)	30 (3/10)	73 (8/11)	0 (0/3)
Ovaries, granulosa cell tumor	50 (4/8)	30 (3/10)	82 (9/11)	33.3 (1/3)
Liver hemangioma	25 (5/20)	50 (8/16)	59 (10/17)	20 (3/15)
Thymic lymphoma	0 (0/20)	12.5 (2/16)	0 (0/17)	6.7 (1/15)
Lung tumors	100 (20/20)	100 (16/16)	100 (17/17)	100 (15/15)

tumor cells (Fig. 9B). In contrast, in the tumors arising in the $p27^{S10A/S10A}$ mice, the $p27^{S10A}$ protein remained predominantly nuclear (Fig. 9B). In these tumors, the complete loss of the p27 protein was never observed, consistent with our immunohistochemistry data (Fig. 9C). However, Ser10 phosphorylation was abundant in tumors from wild-type and $p27^{+/-}$ animals, despite high levels of proliferation as indicated by PCNA levels (Fig. 9C). This is unlike normal tissue, in which Ser10 phosphorylation is abundant only in nonproliferating cells. These data suggest that tumor cells activated a Ser10-dependent pathway that relocated much of the cellular p27 to the cytoplasm.

Urethane-induced lung tumorigenesis has been shown to be caused by mutational activation of K-Ras (Barbin 2000; Meuwissen and Berns 2005), and tumors harvested from our cohort all showed evidence of activation of the Ras pathway, as indicated by increased phospho-ERK1/2 levels (Fig. 9C). It has been reported that active Ras may promote p27 mislocalization to the cytoplasm. However, the importance of Ser10 phosphorylation in the pathway by which Ras induces p27 nuclear export has not been addressed (Liu et al. 2000; Kfir et al. 2005). We therefore compared the subcellular localization of wild-type p27 and $p27^{S10A}$ in MEFs expressing activated K-Ras (Fig. 10). Overexpression of K-Ras V12 caused an increase in cytoplasmic wild-type p27, while it had little or no effect on the localization of $p27^{S10A}$. Most dramatically, Ras-expressing cells treated with the proteasome inhibitor MG-132 accumulated large amounts of wild-type p27 protein in the cell cytoplasm, whereas $p27^{S10A}$ accumulated almost exclusively in the cell nucleus. Thus, Ras-induced cytoplasmic mislocalization of p27 occurred via the Ser10-dependent nuclear export pathway. In sum, our data suggest that the mutation of Ser10 to Ala impairs the Ras-induced nuclear export of p27, thus providing an explanation for the lower tumor burden in $p27^{S10A/S10A}$ mice and for the reduced growth rate of these tumors. Therefore, phosphorylation of Ser10 may constitute an important pathway by which tumor cells modulate the tumor suppressor function of p27.

Discussion

The CDK inhibitor $p27^{Kip1}$ plays a major role in regulating the transition between proliferating and quiescent cell states. In quiescent cells, p27 levels are elevated and then decrease when cells enter the cell cycle, remaining low through the S and G2/M phases. Remarkably, p27 expression is regulated by at least three pathways that mediate its ubiquitin-dependent proteolysis, each of which operates during a unique window of the cell cycle or in a specific subcellular compartment: a nuclear Skp2-dependent pathway that operates in S/G2 and M, and is dependent on phosphorylation of p27 on T187 (Malek et al. 2001; Nakayama et al. 2004); a KPC-dependent pathway that acts in the cytoplasm of G1 cells (Kamura et al. 2004); and a less well-understood pathway that regulates p27 degradation in quiescent cells. There may also be a fourth p27 degradation pathway that acts in the nucleus of G1 cells.

In the present study, we have used two genetically engineered mouse strains to characterize the pathway for p27 degradation that operates exclusively in quiescent cells, and have further shown that misregulation of this pathway is a key mechanism for disrupting p27's tumor suppressor function. $p27^{CK^-}$ mice carry point mutations in the protein interaction domains that are necessary for p27 to bind to cyclins and CDKs (Vlach et al. 1997). In $p27^{S10A}$ mice, the main phosphorylation site on p27 has been mutated to Ala (Ishida et al. 2000). Unexpectedly, we discovered that these mutations together define a single pathway for p27 degradation in quiescent cells.

The $p27^{CK^-}$ protein did not associate with, and therefore did not regulate, cyclins or CDKs, as evidenced by its absence from cyclin and CDK immunoprecipitated complexes, and by the increased growth rate and generalized organomegaly of the $p27^{CK^-/CK^-}$ mice. $p27^{CK^-}$ protein levels were increased in tissues and MEFs, probably because the degradation of $p27^{CK^-}$ was impaired in both G0 and S phases. The increased stability of $p27^{CK^-}$ in S phase was largely expected since transfection experiments had shown that $p27^{CK^-}$ was resistant to cyclin E–CDK2-induced degradation, although it was still a target for phosphorylation on Thr187 by cyclin E–CDK2; indicating a requirement for a stable interaction with cyclin–CDK complexes for efficient turnover in S phase (Vlach et al. 1997; Montagnoli et al. 1999). On the other hand, the dramatically increased stability of $p27^{CK^-}$ in quiescent cells demonstrated that cyclin–CDK binding to p27 is also required for p27 turnover in G0. Thus, the degradation of p27 both in S phase and G0 requires its assembly into cyclin–CDK complexes. In S phase this involves the Skp2–SCF E3-ubiquitin ligase. However,

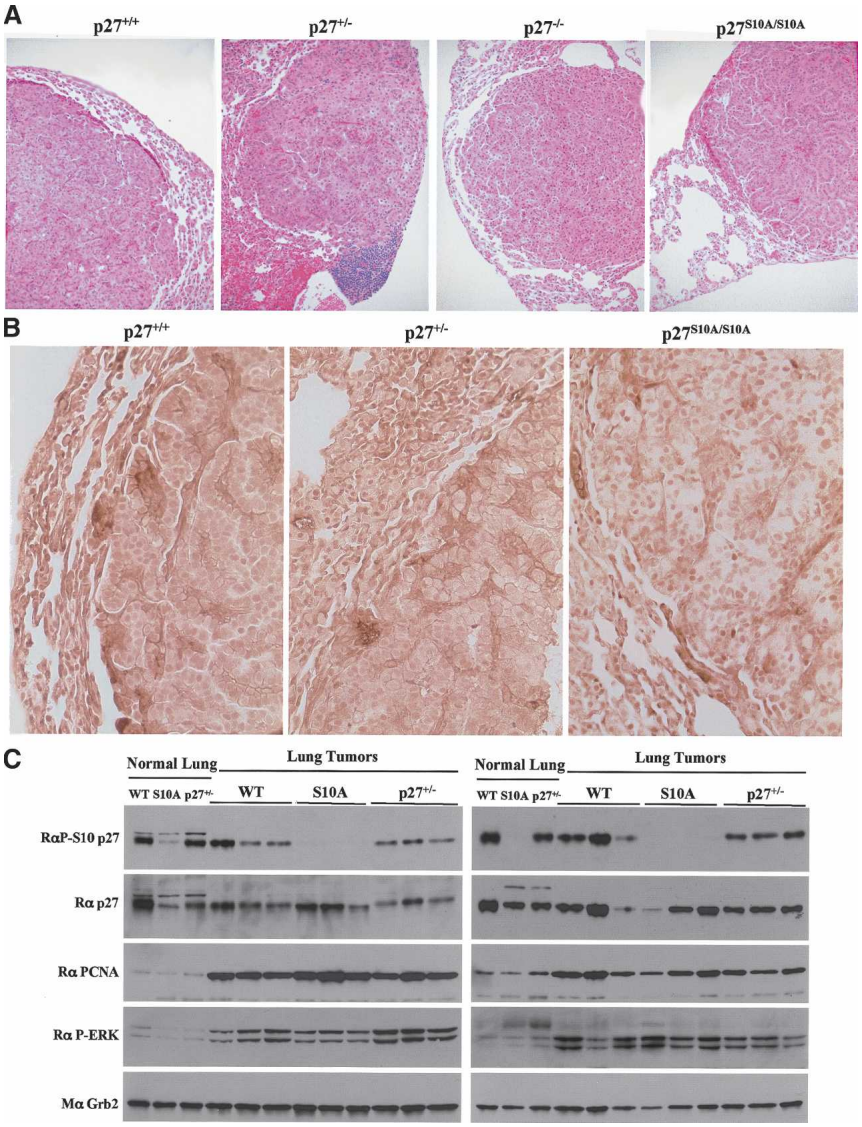

Figure 9. Nuclear localization of $p27^{S10A}$ is maintained in lung tumors. (*A*) Lung tumor histology. Five-micron-thick slices of paraffin-embedded lungs tissues from wild-type, $p27^{+/-}$, $p27^{-/-}$, and $p27^{S10A/S10A}$ mice were stained with eosin and hematoxylin. Tumors were classified as bronchioalveolar adenomas and papillary adenomas. (*B*) p27 immunohistochemistry of lung tumors and normal surrounding tissue. Five-micron-thick slices of paraffin-embedded lung tissues from wild-type, $p27^{+/-}$, and $p27^{S10A/S10A}$ mice were stained using the mouse monoclonal p27 antibody (clone 57; BD-Transduction Laboratories). (*C*) Western blot analysis of normal lung tissue and individual tumors form wild-type, $p27^{+/-}$, and $p27^{S10A/S10A}$ mice. Forty micrograms of proteins were loaded per well. Membranes were probed successively with polyclonal antibodies to phospho-Ser10 p27, p27, PCNA, phospho-ERK (activated), and with a monoclonal anti-Grb2 antibody for protein loading.

the ubiquitin ligase responsible for p27 turnover in G0 is unlikely to use Skp2. Indeed, not only is the recognition motif for Skp2 (phospho-T187) unnecessary for p27 turnover in G0, but also quiescent Skp2-null cells do not express increased amounts of p27 (Nakayama et al. 2000; Hara et al. 2001; Malek et al. 2001). Studies using MEFs lacking specific cyclins or CDKs did not implicate one specific cyclin/CDK complex in p27 degradation in G0. This is not surprising given the very high level of redundancy among different cyclins and CDKs (Pagano and Jackson 2004; Sherr and Roberts 2004), and may thus suggest that any cyclin–CDK complex that can bind p27 can mediate this function. Our data also indicate that these cyclin–CDK complexes do not need to be enzymatically active to promote p27 degradation in G0, possibly providing a structural scaffold for p27 recognition by ubiquitin ligases as reported by others (Zhu et al. 2004). Interestingly, cyclin–CDK binding was dispensable for p27 turnover only during the G1 phase, which may reflect p27 degradation by the cytoplasmic KPC pathway, recently found to mediate the degradation of free p27 (Kamura et al. 2004; Kotoshiba et al. 2005).

Ser10 phosphorylation stabilizes p27 in quiescent cells

p27 stability in quiescent cells is also controlled by phosphorylation on Ser10. The levels of the $p27^{S10A}$ protein were reduced in tissues and MEFs, consistent with its accelerated turnover in G0 compared with wild-type p27. This was in agreement with previously reported transfection experiments, which showed that p27 phosphorylation on Ser10 by the kinase Mirk/Dirk stabilizes p27 in quiescent cells (Deng et al. 2004), and that mutation of Ser10 to Ala or Glu destabilizes or stabilizes p27, respectively (Ishida et al. 2000; Rodier et al. 2001). During the course of this work, Kotake et al. (2005) reported similar findings with regards to $p27^{S10A}$ turnover in a $p27^{S10A/S10A}$ mouse knock-in model.

A central conclusion of our experiments was that dephosphorylation of p27 on Ser10 and assembly of p27

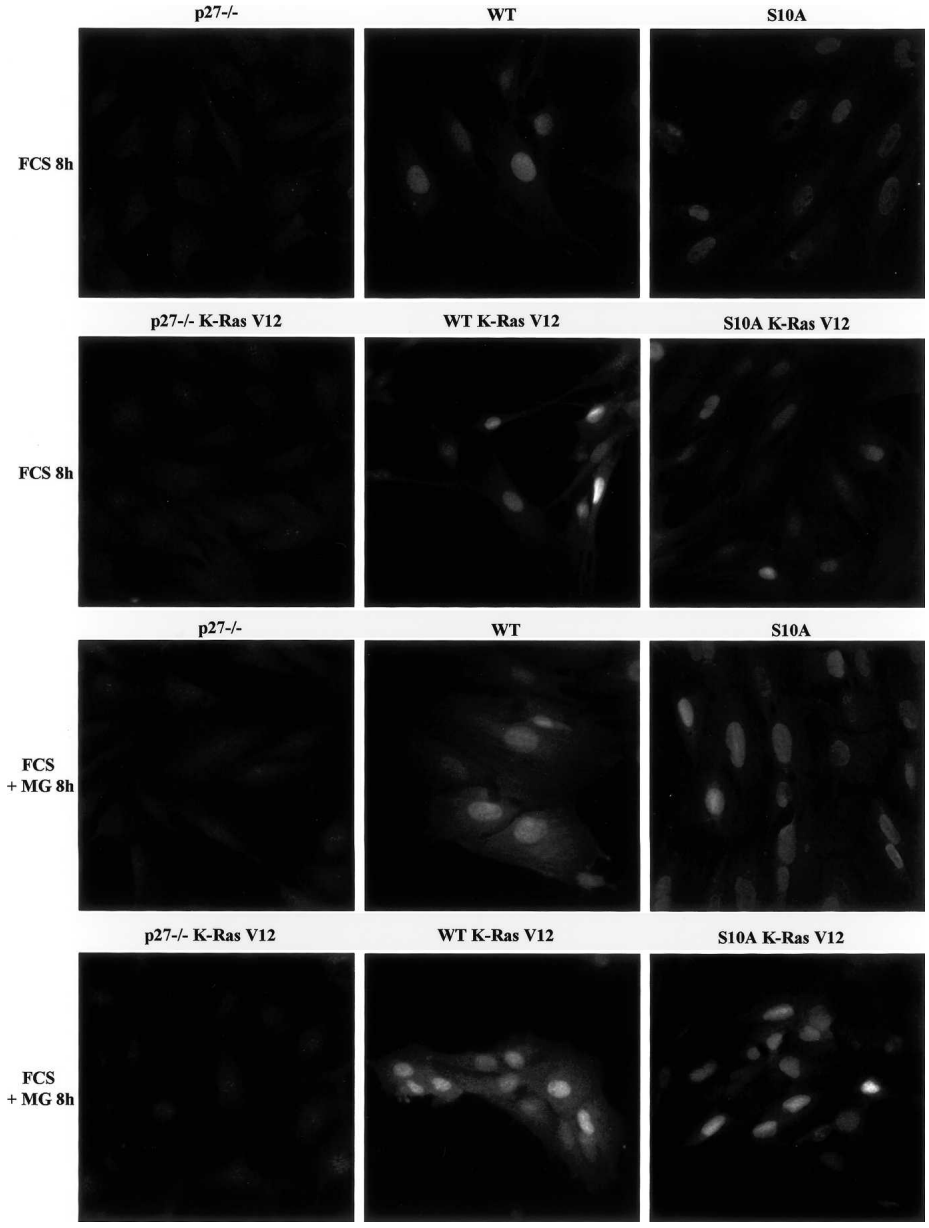

Figure 10. Unlike wild-type p27, $p27^{S10A}$ is resistant to activated Ras-induced cytoplasmic translocation. p27-null, wild-type, and $p27^{S10A}$ MEFs either expressing K-Ras V12 or not were serum starved for 72 h and stimulated with 10% serum in the presence or absence of MG132, fixed, and stained with a monoclonal antibody to p27. As in Figure 7, the exposure time was set on the $p27^{-/-}$ cells (*left* column) and kept constant to acquire all the other images, to take into account the nonspecific signal generated by the antibody.

into cyclin–CDK complexes coordinately regulated p27 stability in quiescent cells, participating in a single turnover pathway. One hypothesis consistent with our data was that dephosphorylation of Ser10 promoted the assembly of heterotrimeric p27–cyclin–CDK complexes, thereby promoting p27 degradation. Indeed, the $p27^{S10A}$ mutation increased the proportion of p27 that was assembled into cyclin–CDK complexes. In accord with this, $p27^{S10A/S10A}$ mice had a normal growth rate and size, and a partial resistance to urethane-induced tumorigenesis, despite having overall reduced amounts of p27 protein. Also, the $p27^{S10A/CK^-}$ double mutant protein was stabilized relative to $p27^{S10A}$, suggesting that p27–cyclin–CDK assembly functioned downstream of Ser10 phosphorylation to control p27 stability.

Nevertheless, if Ser10 phosphorylation controls the interaction of p27 with cyclins and CDKs, it probably does so indirectly. Thus, substitution of Ser10 by the phospho-mimetic amino acid Glu ($p27^{S10E}$) did not inhibit the interaction of recombinant p27 with cyclin–CDK complexes in vitro, even though this same mutation stabilized p27 in vivo. In proliferating cells, Ser10 phosphorylation promotes the interaction of p27 with CRM1, and thereby stimulates its nuclear export (Rodier et al.

2001; Boehm et al. 2002; Ishida et al. 2002; Connor et al. 2003; McAllister et al. 2003; Shin et al. 2005). Export of p27 into the cytoplasm could represent one pathway by which Ser10 phosphorylation indirectly modulates the interaction of p27 with CDKs. Alternatively, Ser10 phosphorylation may control the interaction of p27 with other proteins in quiescent cells that could modulate its interactions with cyclin–CDK complexes.

An alternative hypothesis is that Ser10 phosphorylation directly affects the rate of degradation of p27 within cyclin–CDK complexes. For example, phosphorylation of Ser10 could inhibit p27 ubiquitination by interfering with its recognition by an E3 ubiquitin ligase. Kinetic modeling showed that both hypotheses—an effect of Ser10 phosphorylation either on heterotrimer assembly or degradation of CDK-bound p27—were equally consistent with the observed redistribution of $p27^{S10A}$ into cyclin–CDK complexes, as well as the relative stabilities, abundance, and phosphorylation states of $p27^{S10A}$, $p27^{CK^-}$, and wild-type p27 (F. Cross, pers. comm.). Interestingly, these models showed, in some scenarios, that the free pool of $p27^{S10A}$ becomes depleted because p27 levels are reduced to the point where cyclin–CDK complexes are in excess of p27. Thus, the Ser10 kinase system may regulate p27 through this critical threshold, and thereby ensure that p27 levels in quiescent cells remain in excess of cyclin–CDK complexes.

Ser10 phosphorylation in the regulation of p27 subcellular localization

Mitogenic signals activate a kinase that phosphorylates p27 on Ser10, promotes its interaction with CRM1, and thereby induces its export from the nucleus (Rodier et al. 2001; Boehm et al. 2002; Ishida et al. 2002; Connor et al. 2003; McAllister et al. 2003; Kamura et al. 2004; Shin et al. 2005). In contrast to previous reports, Kotake et al. (2005) concluded that the $p27^{S10A}$ mutation did not inhibit its export into the cytoplasm of MEFs and lymphocytes derived from $p27^{S10A/S10A}$ mice. This is in contradiction with our findings and may reflect technical differences in the way experiments were conducted. When p27-null cells are used as a negative control for immunofluorescence, only small amounts of p27 could be detected in the cytoplasm of wild-type cells above the background staining seen in the $p27^{-/-}$ cells (Besson et al. 2004b). Similar studies with $p27^{S10A}$ MEFs that express reduced amounts of p27 were insufficient to distinguish between a defect in nuclear export or an overall decrease in the amount of $p27^{S10A}$ to below the detection limit of the assay. However, when the pool of cytoplasmic p27 was stabilized by the presence of the proteasome inhibitor MG132, it became clear that export of $p27^{S10A}$ to the cytoplasm was impaired. In addition, when normal lung tissue was compared with a neighboring tumor, wild-type p27 showed a loss of nuclear staining in the tumor but not in the normal adjacent tissue, whereas nuclear staining in $p27^{S10A/S10A}$ tumors was maintained. Thus, $p27^{S10A}$ was a constitutively nuclear protein in cultured cells and in vivo, and was largely resistant to the nuclear export pathway activated by growth factor stimulation and by Ras activation during tumorigenesis. In accord with these observations, we noted high levels of Ser10-phosphorylated p27 in the proliferating cells of lung tumors harvested from wild-type mice. Thus, we find that the nuclear export of p27 is largely impaired by the S10A mutation.

Misregulation of p27 in cancer

Cancer cells frequently exhibit reduced amounts of p27, and this is strongly associated with increased tumor aggressiveness and a poor clinical outcome (Slingerland and Pagano 2000; Philipp-Staheli et al. 2001; Besson et al. 2004a). Increased rates of degradation and elevated rates of nuclear export are thought to cause the decreased nuclear expression of p27 seen in tumor cells, but the specific degradation and nuclear export pathways that are affected are not well understood. For example, increased Skp2-mediated degradation is proposed to cause the lower levels of p27 in tumor cells. However, mice expressing $p27^{T187A}$ (which cannot be degraded by this pathway) are not resistant to lung tumorigenesis, and lung tumors arising in those mice express decreased amounts of p27 similarly to mice expressing wild-type p27 (I. Timmerbeul, C.M. Garrett-Engele, U. Kossatz, X. Chen, E. Firpo, V. Grunwald, K. Kamino, S. Kubicka, M.P. Manns, J.M. Roberts, et al., in prep.). Cytoplasmic localization of p27 in tumor cells can be promoted by Akt-mediated phosphorylation of Thr157 (Liang et al. 2002), but this phosphorylation site is not evolutionarily conserved, and is absent from murine p27.

$p27^{S10A/S10A}$ mice are partially resistant to urethane-induced tumorigenesis compared with mice expressing wild-type p27 protein. Even more dramatic is their resistance to tumorigenesis compared with $p27^{+/-}$ mice, which express an amount of p27 protein that closely approximates that in the $p27^{S10A/S10A}$ homozygote. In our tumorigenesis experiment, $p27^{+/-}$ mice developed more tumors than p27-null animals. Others also reported an increased susceptibility to tumorigenesis of $p27^{+/-}$ mice compared with $p27^{-/-}$ in breast and prostate tumor models, suggesting that the maintenance of reduced amounts of p27 may, in fact, actively promote tumorigenesis (Muraoka et al. 2002; Gao et al. 2004). In contrast, despite its reduced stoichiometry, $p27^{S10A}$ was a better tumor suppressor than wild-type p27. The enhanced tumor suppression by $p27^{S10A}$ correlates with a higher proportion of $p27^{S10A}$ associated with cyclin–CDK complexes than wild-type p27. This may be due to the constitutive nuclear localization of $p27^{S10A}$, which increases its availability to bind to and inhibit cyclin–CDKs. Our data suggest that increased activity of the pathway that phosphorylates p27 on Ser10 may be important during tumor progression, and interfering with this pathway may be a useful therapeutic strategy. The tumor resistance of the $p27^{S10A}$ mice is the first example of a p27 mutation that enhances its tumor suppressor function, and thus constitutes the first direct demonstration of a pathway that is important for misregulation of p27 in cancer.

Materials and methods

Constructs, antibodies, and reagents

The 4317G9 targeting vector was kindly provided by Richard Palmitter (University of Washington, Seattle, WA). The Mox2Cre mice were kindly provided by Philippe Soriano (Fred Hutchinson Cancer Research Center, Seattle, WA). The polyclonal anti-CRM1 antibody was kindly provided by Larry Gerrace (Scripps Research Institute, La Jolla, CA). pBabe-K-Ras V12 was a gift from Channing Der (University of North Carolina, Chapel Hill, NC). Reagents were purchased from the following sources: puromycin and hygromycin (Calbiochem); polyclonal antibodies to p27 (C19), CDK4 (H303), Cyclin D (H295), phospho-Ser10 p27, and monoclonal antibodies to Cyclin D1 (A12), CDK2 (D12), Cyclin E (HE111), PCNA, and p27 (F8) (Santa Cruz Biotechnology); monoclonal antibodies to p27 and Grb2 (BD-Transduction Laboratories); polyclonal antibodies to phospho-p42/44 MAPK (Thr202/Tyr204) (Cell Signaling); pQCXIP and pQCXIH retroviral vectors (BD-Clontech); cycloheximide and MG132 (Sigma); cyanin-3-conjugated secondary antibodies (Jackson ImmunoResearch Laboratories); Alexa 488-conjugated secondary antibodies (Molecular Probes); and horseradish peroxydase-conjugated secondary antibodies (Amersham).

Generation of the knock-in mice

To generate the $p27^{S10A}$ and $p27^{CK^-}$ alleles, a 4700-base-pair (bp) KpnI–EcoRI genomic fragment containing the two coding exons of the *p27* gene was inserted into a pcDNA3.1 vector. Mutagenesis of Ser10 to Ala for the $p27^{S10A}$ allele, and Arg30 to Ala, Leu32 to Ala, Phe62 to Ala, and Phe64 to Ala for the $p27^{CK^-}$ allele was performed using a Quick-change site-directed mutagenesis kit (Stratagene) according to the manufacturer's instructions. Correct mutagenesis of the genomic DNA was verified by direct DNA sequencing. The mutant genomic fragment was then inserted into the 4317G9 targeting vector on one side of the SV40-neo cassette (used as a positive selection marker) flanked by LoxP sites, and a 2800-bp KpnI–XbaI genomic fragment containing the 3′-UTR of the *p27* gene was inserted on the other side of the SV40-neo cassette (Fig. 1A). The coding sequences of the mutant *p27* alleles were sequenced in the final targeting vectors. The herpes simplex virus thymidine kinase (HSV-TK) and diphtheria toxin (DTA) were both used as negative selection markers. Targeting vectors were electroporated into AK7.1 ES cells and after positive and negative selections were applied, and resistant clones were screened by PCR and Southern blot hybridization using a KpnI–HindIII probe containing exon 2 (Fig. 1A). Two correctly targeted clones were used for injection into blastocysts and generation of chimeric mice. Germline transmission was obtained for both clones, and the SV40-neo cassette was removed by crossing $p27^{+/S10A}$ or $p27^{+/CK^-}$ mice with Mox2Cre mice (Tallquist and Soriano 2000). Genotyping was performed by PCR on tail DNA using the following primers: 5′-GCTCCGGTGGGTTAATGAGG-3′ and 5′-CCACGGCAGCTCTATTCACAC-3′.

Tissue culture and retroviral infections

Tissue culture conditions, primary and immortalized MEFs preparation, and retroviral infections were performed as described previously (Besson et al. 2004b).

Immunofluorescence, Western blotting, and flow cytometry

Immunofluorescence and Western blots were performed as described previously (Besson et al. 2004b), except for the phospho-specific antibodies, which were diluted in PBS, 0.1% Tween 20, and 5% bovine serum albumin. Cell cycle profiles by flow cytometry were performed as described previously (Besson and Yong 2000).

Protein half-life determination

For half-life determination in exponentially growing cells, cells were seeded at ~60% confluency in 100-mm plates, grown overnight, and treated with 25 µg/mL cycloheximide for the indicated time. Cells were lysed in 200 µL of 2× sample buffer, sonicated for 10 sec, and boiled. Equal volumes of each lysate were resolved on SDS-PAGE. For half-life determination of other conditions, cells were seeded as above, grown overnight, and serum starved in 0.1% FCS DMEM for 72 h. For half-lives in serum-starved cells, cycloheximide was then added. For G1-phase half-lives, serum-starved cells were trypsinized and replated for 4 h in 10% FCS DMEM prior to cycloheximide treatment. For S-phase half-lives, serum-starved cells were replated in 10% FCS DMEM for 15 h prior to cycloheximide treatment.

Coimmunoprecipitations

Primary MEFs were lysed in IP buffer (50 mM HEPES at pH 7.5, 150 mM NaCl, 1 mM EDTA, 2.5 mM EGTA, 10% glycerol, 0.1% Tween 20; complemented with 1 mM dithiothreitol, 10 mM β-glycerophosphate, 10 mM NaF, 1 mM sodium orthovanadate, 10 µg/mL leupeptin, 10 µg/mL aprotinin, 10 µg/mL pepstatin-A, and 1 mM phenylmethylsulfonylfluoride). Lysates were syringed several times with a $26^{1/2}$-gauge needle. Cellular debris were eliminated by centrifugation for 5 min at 14,000 rpm. Protein concentration was determined using the Bio-Rad protein assay. For each immunoprecipate, 4 µg of the indicated antibody, 500 µg of lysate, 16 µL of protein A sepharose beads (Amersham), and 500 µL of IP buffer were incubated for 3 h at 4°C. Immunoprecipitates were rinsed three times in IP buffer, and 10 µL of 4× sample buffer were added to the bead pellet. The immunoprecipitates were subjected to Western blotting as described previously (Besson et al. 2004b).

In vitro binding and kinase assays

Cyclin E–CDK2 complexes were produced in SF21 cells, and an equal amount of lysate was used in each assay. For the binding assays, 2.5 or 5 ng of recombinant p27 were mixed with 5 µL of cyclin E–CDK2-containing lysate in IP buffer. Cyclin E was then immunoprecipitated with a polyclonal antibody, and the amount of p27 associated with cyclin E was determined by Western blotting. Kinase assays were performed as described previously (Besson and Yong 2000), with a preincubation of the indicated amount of recombinant p27 with a fixed volume of lysate containing the kinase complexes for 15 min at 4°C, and the kinase reactions were incubated for 15 min at 30°C.

Urethane tumor study

$p27^{+/-}$ mice in the 129S4 background were bred to generate the $p27^{+/+}$, $p27^{+/-}$, and $p27^{-/-}$ mice used in the study. Mixed 129S4/C57BL6 $p27^{+/S10A}$ mice backcrossed twice into 129S4 were bred to generate the $p27^{+/+}$, $p27^{+/S10A}$, and $p27^{S10A/S10A}$ animals. A single intraperitoneal injection of urethane (1 g/kg) in pups between 21 and 28 d old was used as a carcinogenic insult. Mice were sacrificed after 20 wk, dissected, and examined for gross lesions of internal organs. Lungs were dissected and photographed with a Nikon Coolpix 5700 digital camera, and lung tumors were counted and their size measured. Lungs were fixed

overnight in formalin, embedded in paraffin, and sectioned for histochemistry (5 µm thickness).

Immunohistochemistry

Lung tissue from wild-type, $p27^{-/-}$, $p27^{+/-}$, and $p27^{S10A/S10A}$ mice was fixed in 4% paraformaldehyde in PBS, processed as paraffin sections, and deparaffinized. p27 immunostaining was performed according to the methods provided in the Immuno-Cruz Staining System Kit (Santa Cruz Biotechnology). Briefly, hydrated tissue sections were steamed for 30 min in 0.1% citrate acid and blocked in serum for 20 min at room temperature. Samples were subsequently incubated with anti-p27 antibody (Rα p27 C19, 1:100 dilution) for 1 h and biotinylated secondary antibody for 30 min, and visualized using the chromogen 3′3′-diaminobenzidine (DAB).

Acknowledgments

We are grateful to Drs. Philippe Soriano, Richard Palmitter, Larry Gerrace, Channing Der, Peter Sicinsky, Kiroaki Kiyokawa, and Philipp Kaldis for providing reagents. We thank Dr. Matthew Fero and the members of the Roberts laboratory for stimulating discussions and advices. A.B. is a Howard Hughes Medical Institute fellow of the Life Sciences Research Foundation. K.S.K.-S. is supported by a National Institutes of Health T32 CA8046 Interdisciplinary Training Grant in Cancer Research. C.J.K. is supported by grants NCI R01 (CA099517) and NIEHS U01 (ES11045). J.M.R. is an investigator of the Howard Hughes Medical Institute.

References

Barbin, A. 2000. Etheno-adduct-forming chemicals: From mutagenicity testing to tumor mutation spectra. *Mutat. Res.* **462:** 55–69.

Besson, A. and Yong, V.W. 2000. Involvement of p21(Waf1/Cip1) in protein kinase C α-induced cell cycle progression. *Mol. Cell. Biol.* **20:** 4580–4590.

Besson, A., Assoian, R.K., and Roberts, J.M. 2004a. Regulation of the cytoskeleton: An oncogenic function for CDK inhibitors? *Nat. Rev. Cancer* **4:** 948–955.

Besson, A., Gurian-West, M., Schmidt, A., Hall, A., and Roberts, J.M. 2004b. $p27^{Kip1}$ modulates cell migration through the regulation of RhoA activation. *Genes & Dev.* **18:** 862–876.

Boehm, M., Yoshimoto, T., Crook, M.F., Nallamshetty, S., True, A., Nabel, G.J., and Nabel, E.G. 2002. A growth factor-dependent nuclear kinase phosphorylates $p27^{Kip1}$ and regulates cell cycle progression. *EMBO J.* **21:** 3390–3401.

Carrano, A.C., Eytan, E., Hershko, A., and Pagano, M. 1999. SKP2 is required for ubiquitin-mediated degradation of the CDK inhibitor p27. *Nat. Cell Biol.* **1:** 193–199.

Coats, S., Flanagan, W.M., Nourse, J., and Roberts, J.M. 1996. Requirements of p27Kip1 for restriction point control of the fibroblast cell cycle. *Science* **272:** 877–880.

Connor, M.K., Kotchetkov, R., Cariou, S., Resch, A., Lupetti, R., Beniston, R.G., Melchior, F., Hengst, L., and Slingerland, J.M. 2003. CRM1/Ran-mediated nuclear export of p27(Kip1) involves a nuclear export signal and links p27 export and proteolysis. *Mol. Biol. Cell* **14:** 201–213.

Deng, X., Mercer, S.E., Shah, S., Ewton, D.Z., and Friedman, E. 2004. The cyclin-dependent kinase inhibitor p27Kip1 is stabilized in G(0) by Mirk/dyrk1B kinase. *J. Biol. Chem.* **279:** 22498–22504.

Fero, M.L., Rivkin, M., Tasch, M., Porter, P., Carow, C.E., Firpo, E., Polyak, K., Tsai, L.H., Broudy, V., Perlmutter, R.M., et al. 1996. A syndrome of multiorgan hyperplasia with features of gigantism, tumorigenesis, and female sterility in p27(Kip1)-deficient mice. *Cell* **85:** 733–744.

Fero, M.L., Randel, E., Gurley, K.E., Roberts, J.M., and Kemp, C.J. 1998. The murine gene p27Kip1 is haplo-insufficient for tumour suppression. *Nature* **396:** 177–180.

Fujita, N., Sato, S., Katayama, K., and Tsuruo, T. 2002. Akt-dependent phosphorylation of $p27^{Kip1}$ promotes binding to 14–3–3 and cytoplasmic localization. *J. Biol. Chem.* **277:** 28706–28713.

Gao, H., Ouyang, X., Banach-Petrosky, W., Borowsky, A.D., Lin, Y., Kim, M., Lee, H., Shih, W.J., Cardiff, R.D., Shen, M.M., et al. 2004. A critical role for p27kip1 gene dosage in a mouse model of prostate carcinogenesis. *Proc. Natl. Acad. Sci.* **101:** 17204–17209.

Hara, T., Kamura, T., Nakayama, K., Oshikawa, K., Hatakeyama, S., and Nakayama, K. 2001. Degradation of $p27^{Kip1}$ at the G0–G1 transition mediated by a Skp2-independent ubiquitination pathway. *J. Biol. Chem.* **276:** 48937–48943.

Hengst, L. and Reed, S.I. 1996. Translational control of p27Kip1 accumulation during the cell cycle. *Science* **271:** 1861–1864.

Ishida, N., Kitagawa, M., Hatakeyama, S., and Nakayama, K. 2000. Phosphorylation at serine 10, a major phosphorylation site of p27(Kip1), increases its protein stability. *J. Biol. Chem.* **275:** 25146–25154.

Ishida, N., Hara, T., Kamura, T., Yoshida, M., Nakayama, K., and Nakayama, K.I. 2002. Phosphorylation of $p27^{Kip1}$ on serine 10 is required for its binding to CRM1 and nuclear export. *J. Biol. Chem.* **277:** 14355–14358.

Kamura, T., Hara, T., Matsumoto, M., Ishida, N., Okumura, F., Hatakeyama, S., Yoshida, M., Nakayama, K., and Nakayama, K.I. 2004. Cytoplasmic ubiquitin ligase KPC regulates proteolysis of p27(Kip1) at G1 phase. *Nat. Cell Biol.* **6:** 1229–1235.

Kfir, S., Ehrlich, M., Goldshmid, A., Liu, X., Kloog, Y., and Henis, Y.I. 2005. Pathway- and expression level-dependent effects of oncogenic N-Ras: p27Kip1 mislocalization by the Ral–GEF pathway and Erk-mediated interference with Smad signaling. *Mol. Cell. Biol.* **25:** 8239–8250.

Kiyokawa, H., Kineman, R.D., Manova-Todorova, K.O., Soares, V.C., Hoffman, E.S., Ono, M., Khanam, D., Hayday, A.C., Frohman, L.A., and Koff, A. 1996. Enhanced growth of mice lacking the cyclin-dependent kinase inhibitor function of p27Kip1. *Cell* **85:** 721–732.

Kotake, Y., Nakayama, K., Ishida, N., and Nakayama, K.I. 2005. Role of serine 10 phosphorylation in p27 stabilization revealed by analysis of p27 knock-in mice harboring a serine 10 mutation. *J. Biol. Chem.* **280:** 1095–1102.

Kotoshiba, S., Kamura, T., Hara, T., Ishida, N., and Nakayama, K.I. 2005. Molecular dissection of the interaction between p27 and KPC, the ubiquitin ligase that regulates proteolysis of p27 in G1 phase. *J. Biol. Chem.* **280:** 17694–17700.

Liang, J., Zubovitch, J., Petrocelli, T., Kotchetkov, R., Connor, M.K., Han, K., Lee, J.H., Ciarallo, S., Catzavelos, C., Beniston, R., et al. 2002. PKB/Akt phosphorylates p27, impairs nuclear import of p27 and opposes p27-mediated G1 arrest. *Nat. Med.* **8:** 1153–1160.

Liu, X., Sun, Y., Ehrlich, M., Lu, T., Kloog, Y., Weinberg, R.A., Lodish, H.F., and Henis, Y.I. 2000. Disruption of TGF-β growth inhibition by oncogenic ras is linked to p27Kip1 mislocalization. *Oncogene* **19:** 5926–5935.

Malek, N.P., Sundberg, H., McGrew, S., Nakayama, K., Kyriakides, T.R., and Roberts, J.M. 2001. A mouse knock-in model exposes sequential proteolytic pathways that regulate

p27Kip1 in G1 and S phase. *Nature* **413:** 323–327.
McAllister, S.S., Becker-Hapak, M., Pintucci, G., Pagano, M., and Dowdy, S.F. 2003. Novel $p27^{kip1}$ C-terminal scatter domain mediates Rac-dependent cell migration independent of cell cycle arrest functions. *Mol. Cell. Biol.* **23:** 216–228.
Meuwissen, R. and Berns, A. 2005. Mouse models for human lung cancer. *Genes & Dev.* **19:** 643–664.
Montagnoli, A., Fiore, F., Eytan, E., Carrano, A.C., Draetta, G.F., Hershko, A., and Pagano, M. 1999. Ubiquitination of p27 is regulated by Cdk-dependent phosphorylation and trimeric complex formation. *Genes & Dev.* **13:** 1181–1189.
Muraoka, R.S., Lenferink, A.E., Law, B., Hamilton, E., Brantley, D.M., Roebuck, L.R., and Arteaga, C.L. 2002. ErbB2/Neu-induced, cyclin D1-dependent transformation is accelerated in p27-haploinsufficient mammary epithelial cells but impaired in p27-null cells. *Mol. Cell. Biol.* **22:** 2204–2219.
Nakayama, K., Ishida, N., Shirane, M., Inomata, A., Inoue, T., Shishido, N., Horii, I., Loh, D.Y., and Nakayama, K. 1996. Mice lacking p27Kip1 display increased body size, multiple organ hyperplasia, retinal dysplasia, and pituitary tumors. *Cell* **85:** 707–720.
Nakayama, K., Nagahama, H., Minamishima, Y.A., Matsumoto, M., Nakamichi, I., Kitagawa, K., Shirane, M., Tsunematsu, R., Tsukiyama, T., Ishida, N., et al. 2000. Targeted disruption of Skp2 results in accumulation of cyclin E and p27(Kip1), polyploidy and centrosome overduplication. *EMBO J.* **19:** 2069–2081.
Nakayama, K., Nagahama, H., Minamishima, Y.A., Miyake, S., Ishida, N., Hatakeyama, S., Kitagawa, M., Iemura, S., Natsume, T., and Nakayama, K.I. 2004. Skp2-mediated degradation of p27 regulates progression into mitosis. *Dev. Cell* **6:** 661–672.
Nourse, J., Firpo, E., Flanagan, W.M., Coats, S., Polyak, K., Lee, M.H., Massague, J., Crabtree, G.R., and Roberts, J.M. 1994. Interleukin-2-mediated elimination of the p27Kip1 cyclin-dependent kinase inhibitor prevented by rapamycin. *Nature* **372:** 570–573.
Pagano, M. and Jackson, P.K. 2004. Wagging the dogma; tissue-specific cell cycle control in the mouse embryo. *Cell* **118:** 535–538.
Pagano, M., Tam, S.W., Theodoras, A.M., Beer-Romero, P., Del Sal, G., Chau, V., Yew, P.R., Draetta, G.F., and Rolfe, M. 1995. Role of the ubiquitin–proteasome pathway in regulating abundance of the cyclin-dependent kinase inhibitor p27. *Science* **269:** 682–685.
Philipp-Staheli, J., Payne, S.R., and Kemp, C.J. 2001. $p27^{Kip1}$: Regulation and function of a haploinsufficient tumor suppressor and its misregulation in cancer. *Exp. Cell Res.* **264:** 148–168.
Polyak, K., Kato, J., Solomon, M.J., Sherr, C.J., Massague, J., Roberts, J.M., and Koff, A. 1994a. p27Kip1, a cyclin–CDK inhibitor, links transforming growth factor β and contact inhibition to cell cycle arrest. *Genes & Dev.* **8:** 9–22.
Polyak, K., Lee, M.H., Erdjument-Bromage, H., Koff, A., Roberts, J.M., Tempst, P., and Massague, J. 1994b. Cloning of $p27^{Kip1}$, a cyclin-dependent kinase inhibitor and a potential mediator of extracellular antimitogenic signals. *Cell* **78:** 59–66.
Rodier, G., Montaglioni, A., Di Marcotullio, L., Coulombe, P., Draetta, G.F., Pagano, M., and Meloche, S. 2001. p27 cytoplasmic localization is regulated by phosphorylation on Ser 10 and is not a prerequisite for its proteolysis. *EMBO J.* **20:** 6672–6682.
Sheaff, R.J., Groudine, M., Gordon, M., Roberts, J.M., and Clurman, B.E. 1997. Cyclin E–CDK2 is a regulator of p27Kip1. *Genes & Dev.* **11:** 1464–1478.
Sherr, C.J. and Roberts, J.M. 2001. CDK inhibitors: Positive and negative regulators of G1-phase progression. *Genes & Dev.* **13:** 1501–1512.
———. 2004. Living with or without cyclins and cyclin-dependent kinases. *Genes & Dev.* **18:** 2699–2711.
Shin, I., Rotty, J., Wu, F.Y., and Arteaga, C.L. 2005. Phosphorylation of p27Kip1 at Thr-157 Interferes with its association with importin α during G1 and prevents nuclear re-entry. *J. Biol. Chem.* **280:** 6055–6063.
Slingerland, J. and Pagano, M. 2000. Regulation of the CDK inhibitor p27 and its deregulation in cancer. *J. Cell Physiol.* **183:** 10–17.
Sutterluty, H., Chatelain, E., Marti, A., Wirbelauer, C., Senften, M., Muller, U., and Krek, W. 1999. p45SKP2 promotes p27Kip1 degradation and induces S phase in quiescent cells. *Nat. Cell Biol.* **1:** 207–214.
Tallquist, M.D. and Soriano, P. 2000. Epiblast-restricted Cre expression in MORE mice: A tool to distinguish embryonic vs. extra-embryonic gene function. *Genesis* **26:** 113–115.
Toyoshima, H. and Hunter, T. 1994. p27, a novel inhibitor of G1 cyclin–CDK protein kinase activity, is related to p21. *Cell* **78:** 67–74.
Tsvetkov, L.M., Yeh, K.H., Lee, S.J., Sun, H., and Zhang, H. 1999. p27(Kip1) ubiquitination and degradation is regulated by the SCF(Skp2) complex through phosphorylated Thr187 in p27. *Curr. Biol.* **9:** 661–664.
Ungermannova, D., Gao, Y., and Liu, X. 2005. Ubiquitination of p27Kip1 requires physical interaction with cyclin E and probable phosphate recognition by Skp2. *J. Biol. Chem.* **280:** 30301–30309.
Vlach, J., Hennecke, S., and Amati, B. 1997. Phosphorylation-dependent degradation of the cyclin-dependent kinase inhibitor $p27^{Kip1}$. *EMBO J.* **16:** 5334–5344.
Zhu, X.H., Nguyen, H., Halicka, H.D., Traganos, F., and Koff, A. 2004. Noncatalytic requirement for cyclin A–cdk2 in p27 turnover. *Mol. Cell. Biol.* **24:** 6058–6066.